European Journal of Pharmaceutics and Biopharmaceutics 128 (2018) 337–362

Contents lists available at ScienceDirect

European Journal of Pharmaceutics and Biopharmaceutics

journal homepage: www.elsevier.com/locate/ejpb

Review article

Recent advances in carrier mediated nose-to-brain delivery of pharmaceutics

Vassilis Bourganis[a], Olga Kammona[b], Aleck Alexopoulos[b], Costas Kiparissides[a,b,*]

[a] Department of Chemical Engineering, Aristotle University of Thessaloniki, P.O. Box 472, 54124 Thessaloniki, Greece
[b] Chemical Process & Energy Resources Institute, Centre for Research and Technology Hellas, P.O. Box 60361, 57001 Thessaloniki, Greece

ARTICLE INFO

Keywords:
Nose-to-brain delivery
Olfactory
Nanocarriers
Transport mechanisms
Computational modeling

ABSTRACT

Central nervous system (CNS) disorders (e.g., multiple sclerosis, Alzheimer's disease, etc.) represent a growing public health issue, primarily due to the increased life expectancy and the aging population. The treatment of such disorders is notably elaborate and requires the delivery of therapeutics to the brain in appropriate amounts to elicit a pharmacological response. However, despite the major advances both in neuroscience and drug delivery research, the administration of drugs to the CNS still remains elusive. It is commonly accepted that effectiveness-related issues arise due to the inability of parenterally administered macromolecules to cross the Blood-Brain Barrier (BBB) in order to access the CNS, thus impeding their successful delivery to brain tissues. As a result, the direct Nose-to-Brain delivery has emerged as a powerful strategy to circumvent the BBB and deliver drugs to the brain. The present review article attempts to highlight the different experimental and computational approaches pursued so far to attain and enhance the direct delivery of therapeutic agents to the brain and shed some light on the underlying mechanisms involved in the pathogenesis and treatment of neurological disorders.

1. Introduction

Neurological diseases, such as Parkinson's or Alzheimer's disease, multiple sclerosis, meningitis, etc., may exhibit distinct pathological and clinical manifestations among patients, but in general encompass a broad spectrum of pathological conditions, which result to alterations in neural function and progressive loss of neural tissue [1,2]. Despite the major advances in both drug delivery research and the understanding of the pathogenesis of neurological diseases, effective treatment options are still missing, presumably due to the complexity of the CNS and the putative multifactorial pathogenic mechanisms. As a result, the currently available therapeutic agents have been generally proven ineffective and mainly aim to attenuate neurodegeneration and moderate the disease progression, but have been unable to reverse it and completely restore normal neural function [1,3,4].

Delivery of drugs to the brain in sufficient quantitites to achieve therapeutic levels is required for the treatment of CNS diseases [5,6]. On the other hand, there are several barriers restricting the delivery of therapeutics to the brain, such as the BBB and the Blood-Cerebrospinal Fluid Barrier (BCSFB) [7,8]. The BBB is located at the cerebral microvasculature level and is critical for maintaining the CNS homeostasis, by allowing the efficient nutrient exchange between the blood and the brain tissue, while precluding the entry of xenobiotics that could impair neurological functions. In fact, it prevents both the paracellular and transcellular transport of hydrophilic, ionized and high molecular weight molecules in the circulating blood due to the complex network of tight junctions (TJs) between adjacent cells and the non-fenestrated capillaries, as well as the diminished pinocytotic activity [6,8–10].

As several higher molecular weight compounds turn out to provide rather promising results on the treatment of CNS disorders, alternative routes for brain administration are constantly explored, which aim to bypass [11] or transiently compromise the integrity of the BBB. The nasal cavity has been employed not only as a portal for the local, but also for the systemic delivery of certain therapeutic agents (e.g., peptides, proteins, stem cells, etc.), due to its large surface area and high degree of vascularization [5,12,13]. Compared to conventional drug delivery approaches, which fall short in overcoming the BBB, intranasal delivery can provide an unprecedented opportunity to administer drugs to the CNS in a targeted and noninvasive manner compared to intracerebroventricular or intraparenchymal injections. This can be achieved by granting direct access to the brain via the olfactory and trigeminal nerve pathways, circumventing this way the BBB and the presystemic gastrointestinal and hepatic elimination [9,13–15]. This drug administration pathway is also associated with enhanced safety, increased patient compliance, ease of administration, rapid onset of action, as well as with minimized systemic exposure [9,12–14].

* Corresponding author at: Chemical Process & Energy Resources Institute, Centre for Research and Technology Hellas, P.O. Box 60361, 57001 Thessaloniki, Greece.
E-mail address: costas.kiparissides@cperi.certh.gr (C. Kiparissides).

https://doi.org/10.1016/j.ejpb.2018.05.009
Received 12 February 2018; Received in revised form 26 March 2018; Accepted 3 May 2018
Available online 04 May 2018

However, despite its numerous advantages, the direct nose-to-brain delivery of therapeutic entities is severely hampered by insufficient bioavailabilities, cytochrome P450-mediated degradation, short retention times, restrictions imposed by the geometry of the nasal cavity (e.g., small volume, limited surface area of the olfactory region, etc.), as well as lack of targeting specificity to the affected area of the brain [7,9,13]. Therefore, the direct Nose-to-Brain delivery has mostly been restricted to the administration of extremely potent molecules [16,17].

Despite the previously mentioned limitations, some promising results have been generated in clinical trials [18–20] and research efforts are still ongoing to render this route an integral part of a viable treatment option. The present review article aims to unravel the transport mechanisms involved in the nasal delivery of therapeutics to the brain, document the existing limitations hindering the direct Nose-to-Brain delivery of medications via the olfactory mucosa as well as the current approaches to enhance drug transport, and summarize the latest advances in carrier development for Nose-to-Brain delivery. Finally, an overview on the various computational methods to investigate the delivery of therapeutic molecules to the brain via the olfactory region is provided, in order to aid towards better understanding this mode of delivery and improve the efficiency of Nose-to-Brain delivery.

2. Configurational parameters pertinent to intranasal administration

The main morphological and structural properties of the nasal cavity are discussed below in order to gain an insight into its elaborate geometry and distinct characteristics related to the Nose-to-Brain delivery of drugs. Thorough understanding of these crucial configurational aspects is essential for the identification of the exact mechanism governing the administration of medications across this pathway, which would in turn take the formulation development to a whole new level by achieving increased therapeutic efficacies and enable the development of successful clinical formulation candidates.

2.1. The nasal cavity

Alongside with the oral cavity, the nasal cavity comprises an external opening for the respiratory system, providing a portal for the entry of air before its subsequent flow to the lower airways. The nasal cavity plays a pivotal role in essential physiological functions, such as humidity and temperature regulation of the inhaled air, particulate and dust filtration and olfaction processes [6,16,21]. From a structural perspective, the nasal septum divides the nose longitudinally into two identical halves [9], each of which is comprised by three different regions, namely the vestibule (with a surface area of ~0.6 cm^2) [22], the olfactory (with a reported surface area of 2–12.5 cm^2 [9,22–24]), and the respiratory regions.

The intricately structured nasal cavity extends approximately 12–14 cm in length [9,21,25] and 5 cm in height [21], while its total surface area and total volume are reported to range between 150 and 200 cm^2 [6,9,24,26] and 13–25 ml [9,16,25,26] respectively. The large surface of the nasal cavity is mainly attributed to three bony structures, namely the superior, the middle and the inferior nasal conchae (or turbinates), which are lined by the highly vascular nasal mucosa and project from the lateral wall of each nasal compartment, playing a major role in the warming, filtering and humidification of the inhaled air [9,24].

During the inhalation process, the air enters through the nostrils into the nasal vestibule and is then directed through the flexible nasal valve (the narrowest aperture of the respiratory tract [23], into the main nasal chamber [21,24]. Cumulative evidence has suggested that only 15–20% of the inhaled air reaches the olfactory region, due to the anatomic configuration of the nasal cavity [23].

As already stated earlier, providing a more detailed overview of the geometrical characteristics and the functions of the nose is not within the scope of this work, which mainly places emphasis on the parameters that are implicated in the intranasal transport of drugs to the brain. Comprehensive review articles on the nasal architecture and precise geometry have been already published [24,27,28].

2.2. The respiratory epithelium

A ciliated pseudostratified columnar epithelium, called respiratory epithelium or Schneiderian membrane, lines the respiratory region, which occupies the greatest part of the nasal cavity (~80–90% of the total surface area [9,16,22]. The respiratory epithelium (Fig. 1a) is the major site for systemic drug absorption, primarily due to its large microvilli-covered surface area and its high degree of vascularisation [16,23,29]. In fact, it receives its blood supply from an arterial branch of the maxillary artery [29].

From a cellular composition perspective, the respiratory epithelium is comprised by four morphologically distinct cell types, namely the ciliated and non-ciliated columnar cells, the basal cells and the goblet cells, whose main functions lie in the coordinated sweeping motion of the cilia, the water and ion exchange between cells, the process of mucus secretion and clearance as well as the regulation of the humidity of the mucosa [6,22].

The respiratory epithelium is covered by a double-layered mucus gel, consisted of the low viscocity pericilliary layer, which extends 3–5 μm in thickness and surrounds the motile cilia (2–4 μm in length) and the overlying viscous gel layer, which extends 2–4 μm in thickness [23,30,31]. The respiratory mucus is a viscoelastic gel, composed of a network of high molecular weight glycoproteins called mucins, water, salts, other proteins and a small fraction of lipids, and serves as a protective barrier due to its viscoelastic and adhesive properties and represents the first line of defense against inhaled particulates and irritants [32–34]. The thickness of the low viscocity serous fluid layer is determined so that the sweeping motion of cilia occurs within the low viscosity fluid, with only the cilia tips brought into contact with the viscoelastic mucus gel layer [31]. This particular ability of the cilia to perform a coordinated sweeping movement with a frequency of approximately 1000 S/min [23], translates into mucus shedding by vectorial propulsion towards the pharynx, which, along with the continuous mucus secretion process, results to mucociliary clearance, that exerts its protective effect by entrapping and removing inhaled particulates, irritants and microbes, which are transported posteriorly with an approximate rate of 1–30 mm/min [24] until they get inactivated by acid- and enzyme-mediated lysis in the stomach [6,16,23,31]. This can lead to the rough estimation that the respiratory mucus layer is renewed every 10–20 min [25,35].

2.3. The olfactory epithelium

The olfactory system has attracted significant scientific interest among the components of the nasal cavity, due not only to the ability of its neurons to detect odorants and provide the sense of smell, but also for its ubiquitous ability to provide a portal for direct delivery of medications to the brain.

From a structural perspective, the olfactory mucosa (Fig. 1b) consists of a ciliated chemosensory pseudostratified columnar epithelium and is situated on the superior turbinate and bilaterally on the nasal septum, while it is completely surrounded by respiratory epithelium. The olfactory mucosa also involves the lamina propria, which is located beneath the epithelial basement membrane and apart from a dense capillary network, contains lymphatic vessels, olfactory axon bundles, autonomic nerve fibers, the maxillary branch of the trigeminal nerve and the mucus-secreting Bowman's glands, which account for the secretion of the overlying mucus gel layer [22,26].

In contrast to the respiratory epithelium, the olfactory mucosa receives its blood supply from ophthalmic artery branches [29], and the cilia of the olfactory epithelium are longer (i.e., over 50 μm [22] and

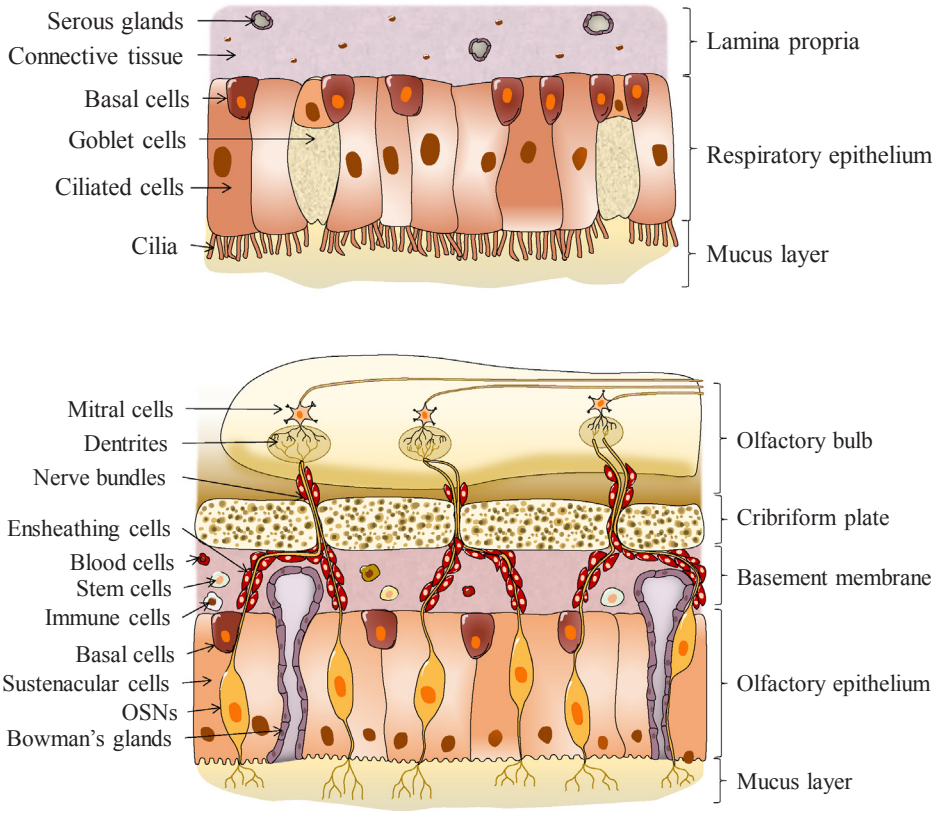

Fig. 1. Two distinct types of pseudostratidfied epithelia located in the nasal cavity: (a) the respiratory epithelium, which lines the upper airways and is mainly comprised by goblet, basal and ciliated cells and (b) the olfactory epithelium located on the roof of the nasal cavity, which mainly containins the ciliated receptor neurons, the basal and the sustenacular cells.

non-motile. However, despite the lack of motion, mucus clearance is still feasible, presumably due to continuous mucus secretion and shedding due to gravitational and mechanical forces as well as due to a solvent drag effect, although the overlying mucus gel exhibits a very slow turnover, in the order of several days [6,7,24]. Defense mechanisms also include the secretion of xenobiotic-metabolizing enzymes and antibodies of the immune system [36]. The importance of the mucus defensive mechanisms is obvious in disease state, where olfactory acuity is considerably decreased as the clearance is notably obstructed due to the increased mucus viscosity [36].

Although there exist significant variations in the reported values, the olfactory region in humans occupies 2–12.5 cm^2, which represents a minor fraction of the total surface area of the nasal cavity (approximately 1.25–10%) [9,22–24], while it is around 60 μm thick [22]. It should be noted that the exact morphology and structure (e.g., olfactory surface area, cellular composition) of the olfactory system and related structures may vary significantly among species (see Table 1), which reflects the major differences in the sensing ability and olfaction between human subjects and other species [16,24,36].

Several distinct cell types can be identified in the olfactory epithelium, while the overlying mucus gel is secreted by the Bowman's glands, situated throughout the epithelium [36]. The mucus gel layer varies in thickness between the different species (Table 1), and performs its function by cleaning the sensory structures and solubilizing odoriferous substances, while it is also capable of entrapping foreign entitites [22].

Sustentacular cells represent the most abundant cell type of the olfactory epithelium. They are columnar cells that posses microvilli and provide metabolic and mechanical support to the olfactory epithelial cells [9,22], while also regulating the ionic environment of the overlying mucus gel. They exhibit high enzymatic activity imparted by cytochrome P-450, etc., thus catabolizing inhaled xenobiotics [24]. The basal cells are small, conically-shaped cells [26], located in the basement membrane. Apart from providing mechanical support to other cells [6], their multipotent nature renders them capable of differentiating into other cell types (e.g., sustentacular cells, cells of the Bowman's glands, and olfactory sensory neurons (OSNs) in particular), thus continuously replacing deceased cells [9]. The microvilli-possessing brush cells also reside in the olfactory epithelium, constituting the terminal branches of the trigeminal nerve. Their primary function lies in the sensation of sensory stimulation of the mucosa [22]. Microvillus cells are also present in the olfactory epithelium, although their exact role remains unknown [9]. However, the OSNs represent the most important cell type of the olfactory epithelium. They comprise a bipolar cell type, interspersed among the sustentacular cells [26], which is responsible for the odorant reception and the transduction of chemical stimuli into neural signals, which is the basis of the process of olfaction. OSNs possess dendrites at their apical surface that extend into an enlarged knob protrusion with several non-motile cilia, which project into the overlying externally exposed mucus gel [9,36]. At its basal surface, OSNs bring about unmyelinated axons that transmit olfactory signals and bundle together to form thick axon bundles, which are enclosed by the olfactory ensheathing cells and olfactory nerve fibroblasts and may enter the cribriform plate of the ethmoid bone through its foramina. The ensheathed unmyelinated axon bundles comprise the olfactory nerve, which extends up to the dendrites in the glomeruli of the olfactory bulb, which is in turn inhabited by the tufted and mitral cells, and penetrate further into the brain [9,16,22].

Table 1
Surface area of olfactory epithelium and thickness of olfactory mucus layer.

Species	Mucus thickness (μm)	Olfactory epithelium surface area (cm^2)
Mice		1.25–1.40 [16]
Rats	2.8 [37]	4.2–6.8 [9,16]
Rabbits	≥3 [38]	
Dogs	10 [39]	170–380 [16]
Humans	60 μm thick [22]	10 [16]
	Varying thickness [40]	2–12.5 [9,22–24]

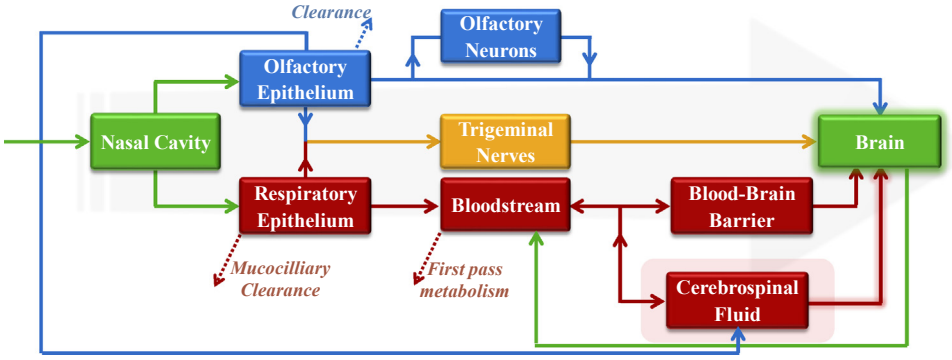

Fig. 2. The potential transport pathways followed by therapeutic agents after intranasal administration.

3. Pathways & mechanisms for nose-to-brain delivery

Although the direct transport of several therapeutic entities to the brain through the nasal cavity has been the topic of numerous research studies, only a small fraction of the initial medication dose can in fact reach the brain, which in turn suggests that the exact pathways and underlying mechanisms still remain elusive. A brief overview of the mechanisms/pathways governing the intranasal delivery of therapeutics to the CNS is, therefore, provided below, along with strategies that could be applied to circumvent current limitations and increase the drug concentration in the brain at levels capable of eliciting a pharmacological response. Identification of the exact mechanisms governing intranasal drug delivery to the brain would enable the development of optimized galenic formulations and revolutionize the therapy of CNS diseases.

Although still speculative, the precise mechanisms involved in the Nose-to-Brain delivery of drugs have been well-documented and several direct and indirect transport pathways have been proposed, according to which, the Nose-to-Brain transport occurs mainly via the (i) systemic, (ii) olfactory and (iii) trigeminal nerve pathways [5,17,23,41].

The common feature between these distinct pathways is that they all presuppose the intranasal delivery of medications and the (partial) avoidance of elimination due to enzymatic degradation or the physical clearance mechanisms [5]. However, they differ entirely regarding the drug absorption site and the amount of time required for absorption to occur. The dominance of a certain pathway over the others is principally dictated by the physicochemical properties of the drug (or the formulation) and the application method [29]. The several transport pathways are illustrated in Fig. 2 and are separately discussed below.

3.1. The systemic pathway

The systemic pathway represents an indirect route for nose-to-brain delivery and involves the direct absorption of the drug (or drug-loaded formulation) from the highly vascular nasal respiratory epithelium and the lymphatic system, and its subsequent transport into the systemic circulation [5,23]. Prior to its systemic absorption, the drug should enter the nasal cavity and resist the enzyme- and mucociliary clearance-mediated elimination processes [5], while accordingly it has to cross the BBB in order to reach the brain parenchyma [29,41]. It should be noted however, that the systemic pathway mainly accounts for the transcellular delivery of low molecular weight lipophilic substances that can be more readily absorbed into the bloodstream, exhibiting a profile resembling that of an intravenous injection [10], and subsequently cross the BBB to enter the brain parenchyma [23]. Depending on their molecular weight, the observed bioavailabilities for more hydrophilic molecules, which follow the aqueous paracellular route, range between < 1–10%, where higher bioavailabilities correlate with lower molecular weights [26]. Other factors that may also facilitate the permeation of the drug across the BBB are the net positive charge or certain molecular structures and shapes [42,43].

Apart from the BBB and its related drawbacks (e.g., short circulatory half-lives of drugs, drug binding to plasma proteins thus retarding uptake, unfavorable pharmacokinetics, major differences in the integrity of the blood-brain barrier among subjects and disease states, as well as certain molecular and physicochemical characteristics that render the drugs incapable of crossing the BBB [5,42]), the systemic pathway is also associated with hepatic- and renal-induced drug metabolism, increased systemic exposure and lack of specificity for brain tissues which potentially results in accumulation in other tissues and toxic side effects [29].

A cumulative amount of evidence also suggests that the transfer of drugs from venous to carotid arterial blood supply and subsequently to the brain via a local counter-current mechanism poses another subset of the systemic pathway [29,44]. It should be noted, however, that this pathway remains the least explored and relevant studies have been carried out solely in animal models (e.g., rabbits [45], rats [46,47], swine [48] and sheep [44], and not in humans.

Gaining access to the systemic circulation does not necessarily correspond to the successive direction of the drug towards the BBB, regardless of its ability to cross it. Drug transfer from blood to the brain can alternatively occur across the choroid plexus, where the drug will initially enter the cerebrospinal fluid (CSF) at a rate inversely related to its molecular weight, and may subsequently diffuse into the brain tissue, although in minor quantities, due to a slow, diffusion-driven permeation process [49,50]. It is noteworthy that the transport to the CSF from the bloodstream is unidirectional, since the CSF is subsequently drained into the peripheral bloodstream, approximately every 5 h [26].

3.2. The olfactory pathway

As already mentioned, the transport through the olfactory mucosa has been widely explored as a promising approach to efficiently deliver therapeutic entities from the nasal cavity to the CSF or brain tissue for the treatment of CNS diseases, while simultaneously allowing for the more prompt onset of action, reduced systemic exposure and ability to bypass the BBB. Indeed, the absorption of the drugs along the olfactory region accounts primarily for their high exposure in the CNS, CSF and olfactory bulb [16].

The olfactory pathway can be further subdivided into the neuronal and the epithelial routes [16,17,51], while another classification may occur with respect to the extracellular or intracellular fate of the delivered substances [29,41].

Along with the trigeminal nerves, the olfactory neurons play a fundamental role for brain-targeted drug delivery [41]. The neuronal route is characterized by the internalization of drugs or drug-containing formulations into the olfactory sensory neurons by endocytotic or pinocytotic mechanisms and their intracellular axonal transport along the neurons into the olfactory bulb, wherefrom they are further distributed

throughout the CNS [17,23,52], since several neural projections exist there that extend to certain brain regions (e.g., the ollfactory tract, the piriform cortex, the hypothalamus, etc.) [29]. Human olfactory axons have a typical diameter of 0.1–0.7 μm [53], which in turn suggests that only entities within such dimensions will be able to be transferred along this pathway.

The axonal transport of certain elements or substances has been the subject of numerous studies [54–60]. In particular, Gottofrey and coworkers [57] studied the transport of radiolabeled cadmium ($^{109}CD^{2+}$) along the olfactory region of northern pikes, suggesting a transport along the olfactory neurons. Accordingly, Thorne and coworkers quantitatively studied the transport mechanism of an intranasally administered wheat germ agglutinin-horseradish peroxidase (WGA-HRP) conjugate, suggesting the protein uptake into the olfactory nerves and its transport along the olfactory sensory neurons into the brain. However, it should be noted that this study was a time-consuming one, and the WGA-HRP administration had a total duration of 48 h, suggesting a presumably slow transport mechanism [58]. In a more recent study by the same group [59], Thorne and coworkers demonstrated that the delivery of IGF-I to the rat brain can also be effected via axonal transport. Kristensson et al [55] also performed a quantitative study with long-nosed garfish, demonstrating that inhaled proteins can be indeed taken up by sensory cells. In another experimental study, the transport pathways of wheat germ agglutinin conjugated polyethylene glycol-polylactic acid (PEG-PLA) nanoparticles (WGA-NP) have been investigated, showing that the olfactory neuronal pathway is involved in the delivery of the nanoparticles to the brain tissue [61].

A common finding in most of these studies was that the mechanism of axonal transport is rather slow and inefficient, requiring a considerable amount of time for a drug to reach the CNS [10,16,29,62]. However, faster transport rates are also reported in the literature [54,56,57,60], suggesting that the transport velocities may be significantly affected by other factors, such as the transported substance, the species, the axon diameter, etc [54,57,63].

Delivery of medications to the brain via the olfactory region may also be effected via the olfactory epithelium, as already demonstrated for insulin [64], nerve growth factor (NGF) [65], dihydroergotamine [66], lidocaine [67,68], etc. However, only a few articles have shown the transport of nanoparticles (NPs) via the olfactory epithelial pathway [10,61,69]. The epithelial pathway appears to be considerably faster compared to the axonal transport, with drugs requiring only several minutes upon intranasal administration to reach the olfactory bulb and other brain regions [10,29,70]. The transport across the olfactory mucosa involves both intracellular and extracellular mechanisms. The permeation of the mucus gel layer as well as the underlying epithelia is essentially required, which can be effected either via the transcellular route (by means of receptor-mediated endocytosis or passive diffusion through the membrane of the sustenacular cells and the cells comprising the Bowman's glands) or paracellularly (through the tight junctions between adjacent neural and/or supporting cells) [9,23,25]. Several assumptions have been made regarding the exact process that materials enter the perineural spaces, suggesting that extracellular transport occurs either through the leaky, loosely adherent epithelium surrounding the olfactory nerves or by paracellular diffusion to the underlying lamina propria [9,10,16]. Other transport mechanisms likely involve extracellular convection (bulk flow) and diffusion within perineuronal channels, perivascular spaces or lymphatic channels being in direct connection with the brain tissue or the cerebrospinal fluid [29,52]. After reaching the lamina propria, the drugs may further enter the spaces neighboring the olfactory neurons and get access to the CNS [41,51].

While the transcellular pathway is mainly relevant for the rigorous transport of more lipophilic entities, the absorption of more hydrophilic drugs is carried out by a slow, passive diffusion-driven process through aqueous, fluid-filled channels and exhibits an inverse relation to the molecular weight of the drug [25].

3.3. The trigeminal nerve pathway

The trigeminal nerve route represents an alternative, less explored pathway to the brain and utilizes the branches of the trigeminal nerves, which innervate both the respiratory and olfactory mucosa, as a conduit for the delivery of drugs (or their formulations) to the brainstem and other connected structures [5,71,72]. The trigeminal nerve is the largest cranial nerve and its main function lies in the conveying of chemosensory and thermosensory information to the oral, ocular and nasal mucosae [6,73,74]. Although the trigeminal nerve fiber endings are not directly exposed in the nasal cavity, it is assumed that the initial point of entry is likely from branches (e.g., ophthalmic and maxillary) of the trigeminal nerve, which innervate the dorsal nasal mucosa along with the anterior part of the nasal cavity and the lateral walls of the nasal mucosa respectively [23,29]. Along with the mandibular branch, the three branches of the trigeminal nerve synapse at the trigeminal ganglion and enter the brainstem at the pons level, before subsequently been directed to the rest of the hindbrain and forebrain [5,6,23].

As in the previously discussed case of the olfactory neurons, transport via the trigeminal pathway may occur either intracellularly or extracellularly [9,70,75]. Several studies have been published regarding the axonal transport of various agents (e.g., Insulin-like growth factor 1 (IGF-1) [59], lidocaine [71], Interferon-β-1b (IFNβ-1b) [76], WGA-HRP [77], etc.) through the trigeminal nerves following intranasal administration.

3.4. The lymphatic pathway

The submucosal area of the olfactory region (lamina propria) presents many extracellular pathways for drug transport. A drug can be transferred via extracellular pathways (e.g., perineural, perivascular or lymphatic channels) associated with olfactory nerve bundles extending from the lamina propria through the cribriform plate into the olfactory bulb of the brain. Alternatively a drug can be cleared from the lamina propria by absorption into olfactory blood vessels or into olfactory lymphatic vessels which drain into the deep cervical lymph nodes in the neck. Although the exact pathways are still unclear it has been established that there is a connection between the subarachnoid space, nasal mucosa, and deep cervical lymph nodes [9,78].

3.5. Modulating the affinity to a certain pathway

Although the paracellular pathway is mostly reported to predominate over the others [6], numerous factors influence the delivery of drugs to the brain and may potentially determine which of the aforementioned pathways may predominate in terms of the extent of drug absorption. It is, however, difficult to distinguish which of the pathways prevails every time and it is possible that all three pathways contribute either independently or in a synergistic manner to the transport of therapeutics.

It is commonly accepted that the affinity of a therapeutic to a certain pathway is notably modulated by either its own, or the formulation properties, such as the size (of the primary particle or the agglometrate [62]), lipophilicity, molecular weight, concentration, surface charge, etc., which may ultimately dictate the exact pathway that will be followed [26]. However, the exact pathway for each separate substance remains difficult to identify, let alone to predict and more mechanistic studies are therefore required to provide solid evidence on the exact contribution of the aforementioned parameters. Still, it is considered that intracellular and axonal transport routes do not likely predominate, since the short time intervals between the intranasal administration and the detection to the brain are more consistent with the rapid extracellular transport mechanisms [6,23,29,70]. In addition, since the systemic route is associated with rather significant problems (e.g., increased systemic exposure, short circulatory

half-lives, unfavorable pharmacokinetics, inability of certain drugs/formulations to cross the BBB, etc [5,42]), targeting the olfactory epithelium might be pursued.

In conclusion, research efforts should focus on advanced predictive tools and formulation technologies to direct the drug delivery systems to the desired pathway, enhance the delivery rates and enable the efficient and trouble-free intranasal delivery to the brain.

4. Approaches to enhance drug absorption to the brain via the nasal cavity

As previously discussed, the distinct characteristics of the nasal cavity (e.g., high enzymatic activity, rapid physical clearance mechanisms, poor mucosal permeability, drug deposition-related problems due to the structural complexity of the nasal cavity, etc.) all restrict the efficient delivery of pharmaceutics to the brain in therapeutic relevant quantities. Both conventional and non-conventional approaches have been pursued so far to ease the transport of therapeutic molecules to the brain via the nasal cavity, including the introduction of chemical modifications to the drug molecules, utilization of auxiliary agents either as formulation components or as co-administration agents, as well as formulation development approaches (i.e., micro- or nanoparticulate systems), which can act as CNS-targeting delivery platforms, providing a stability-enhancing effect on the therapeutic agents, while also allowing for increased mucosal permeability. A brief description of the existing strategies to promote the absorption of medications through the nasal cavity is provided below.

4.1. Chemical modification of therapeutic agents

An interesting approach to enhance stability, regulate protease susceptibility and improve membrane permeability and absorption of active compounds is to chemically modify their structure, thus altering their properties [35,79]. Chemical modifications (e.g., use of prodrugs, cyclization, PEGylation, lipidization, amino acid substitutions, etc.) [80,81] aim to alter (or inherit) certain properties of a therapeutic agent on a case by case basis, in order to optimize its properties for the intended purpose. For example, targeting-specificity may be inherited by means of chemical modifications and surface functionalization [82], whereas hydrophilicity/hydrophobicity modulation may be effected by means of lipidization [83,84], PEGylation [85–88], or amino acid substitution [89].

4.2. Enzyme inhibitors

It is well known that the nasal cavity, including the olfactory region, exhibits a markedly high mucosal protease and reductase activity since it plays a host for several drug-metabolizing enzymes (e.g., CYP-450 isomers, oxidative and conjugative enzymes, exo- and endopeptidases, etc.) [35,90–92]. As a result, the enzymatic environment leads to the degradation and metabolism of certain drugs (i.e., mainly protein therapeutics) that employ the nasal cavity as the portal of entry into the body, leading to a “pseudo” first-pass effect [35] and suggesting that the penetration barrier is not the sole reason for the limited absorption [93].

The inclusion of protease-inhibiting agents, either as formulation excipients or as co-administration agents, has been proposed as a viable means to overcome the enzymatic barrier of the nasal cavity [90,92–97], along with other approaches, such as formulation-based techniques (i.e., micro- or nanoparticulate systems), as well as modulation of the surrounding pH, which directly correlates with the regulation of the protease activity [79]. In particular, enzyme inhibitors can potentially enhance the stability of labile therapeutics at the absorption site by inhibiting their enzyme-induced degradation [98].

4.3. Permeation enhancers

Permeation or absorption enhancers have been recommended as one of the most versatile functional formulation excipients that increase and optimize the permeability of therapeutic entities across biological membranes. They are, in general, low molecular weight agents that transiently promote the absorption of therapeutics in pharmacologically active quantities [79,93,99].

Various compounds have been identified to exhibit permeation-enhancing properties (e.g., fatty acids, cyclodextrins, hydrophilic polymers, surfactants and bile salts) [35,99] and classification may occur into various distinct subclasses, with chelating agents, fatty acids as well as synthetic, semi-synthetic or naturally-derived surfactants being the most commonly utilized [93].

Permeation enhancers may exert their absorption-promoting effects through discrete mechanisms that aim to either modify the membrane permeability (i.e., transient disruption of the junctional complex structures between adjacent epithelial cells, interaction with the phospholipid membrane, or increase of its viscoelastic properties) or the properties of the medication itself (i.e., by altering its thermodynamic activity) [79,93,100].

For nose-to-brain delivery applications, permeation enhancers should ultimately aim to alter the extent of transport across the nasal membrane by primarily targeting the olfactory epithelium, wherefrom the medication will be further directed towards the olfactory bulb and the CNS [16,100]. In that case, the regulation of the paracellular porosity by the reversible opening of the tight junctions seems to be the most relevant approach to facilitate the absorption of polar, hydrophilic compounds (e.g., proteins) which are unable to permeate the cellular membrane [7,79,100]. The absorption-promoting capacity of various permeation enhancers in the intranasal delivery of certain therapeutics has been demonstrated in various studies [101–103], while a comprehensive overview on the absorption enhancers for nasal delivery applications has been published by Davis et al [100].

Nevertheless, extreme caution is required regarding the utilization of permeation enhancers as auxiliary agents, since critical parameters should be carefully considered and well controlled (i.e., toxicity, interpatient variability, inadvertent transport of other molecules, as well as difficulty in the extrapolation of data from animal studies to humans) [79,104].

4.4. Vasoconstrictors

Vasoconstrictors have been conventionally employed as nasal decongestants. Their mechanism of action briefly involves the constriction of dilated blood vessels, thus increasing blood pressure, reducing swelling and relieving the nasal congestion symptoms [27]. Utilizing vasoconstrictors as auxiliary agents during formulation development or prior to the drug/formulation administration has been proposed to reduce the amount of drug absorbed into the systemic circulation via the respiratory epithelium, providing this way higher targeting specificity to the CNS through the olfactory pathway, and also diminishing adverse effects related to high systemic exposure [7,16,105]. In fact, Dhuria et al provided solid evidence that the incorporation of the short-acting vasoconstrictor phenylephrine into hypocretin-1- or L-Tyr-D-Arg-containing nasal formulations resulted into diminished systemic exposure and enhanced brain targeting specificity [50]. Contradicting studies also exist in the literature [106], where a solution of the vasoconsticting agent ephedrine increased both the systemic and CNS uptake of the radiolabeled GR138950 model drug compound. However, it was later postulated by Mistry et al that the observed discrepancies between the two studies could be attributed to the longer onset of action of ephedrine, compared to the faster-acting phenylephrine [6].

4.5. Efflux transporters

Efflux transporters have been rarely mentioned concerning drug transport through the nasal mucosa [107,108]. However, it has been lately shown that the co-administration of rifampicin (i.e., P-glycoprotein efflux inhibitor) resulted in increased drug uptake in the brain. Still, further studies are necessary to indicate any potential role of the P-glycoproteins present in the olfactory epithelium on the enhancement of drug uptake in the CNS [27].

4.6. Mucoadhesive agents

Mucoadhesive agents (e.g., polymers exhibiting mucoadhesive properties like chitosan, pectin, carbopol, polacrylic acid, etc) have been also applied as nose-to-brain delivery enhancers, being employed either as formulation excipients or as co-administration agents. Their mechanism of action stems from the fact that mucoadhesives interact with mucus and increase drug residence time in the nasal cavity, thus facilitating absorption. However, despite the lack of motile cilia at the olfactory mucosa, mucociliary clearance still occurs due to gravitational forces and the continuous secretion of mucus by the Bowman's glands [7,16,30]. Mucoadhesives could also act by facilitating the fluidization of the mucosal membrane, thus increasing its permeability [16].

Carbopol, polyacrylic acid and carboxymethylcellulose were found to improve the pharmacokinetics of nasally administered apomorphine whereas hyaluronic acid enhanced the brain transport of a therapeutic peptide, while chitosan also gnificantly improved the brain bioavailability of a nerve growth factor. Enhanced targeting of buspirone hydrochloride was also achieved by combining chitosan hydrochloride with hydroxypropyl β-cyclodextrin as mucoadhesive agents. Finally, a thermosensitive gel consisting of chitosan and hydroxypropylmethyl cellulose, that can be formed *in situ*, improved the brain delivery of a dopamine D2 agonist [105]. However, it should be mentioned at this point that mucoadhesive polymers do not preferentially adhere to the olfactory epithelium and thus, a combination of mucoadhesives with an appropriate targeting ligand would be more efficient to achieve Nose-to-Brain delivery of pharmaceutics [16].

4.7. Nasal delivery devices

Significant progress has been observed in the development of efficient nasal delivery devices appropriate for Nose-to-Brain delivery of therapeutic agents [28,109,110]. Such delivery devices employ versatile technologies to direct the flow and optimize the deposition of the drug (either in powder, particulate or aerosol form) to the upper part of the nasal cavity. The nasal devices include, but are not limited to, powder inhalers, nebulizers, sprays atomizers etc. Kurve Technology©, for example, has developed a Controlled Particle Dispersion® Technology which, among other applicatins, is suitable for direct Nose-to-Brain delivery. Nasal delivery devices, like the ViaNase electronic atomizers, incorporating this technology have been shown to achieve Nose-to-Brain transport via the olfactory region in clinical trials. More specifically, statistical improvement was observed in AD patients in a Nose-to-Brain clinical trial [111]. Mystic Pharmaceuticals© acquired a US patent (US Patent 9,248,076 B2) [112] for its Dose Dispensing Containers which permit the company to efficiently contribute to the non-invasive Nose-to-Brain delivery of small molecule drugs and biomolecules for the treatment of neurodegenerative disorders [113]. Impel NeuroPharma©'s POD™ nasal drug delivery platform (US9550036 B2) [114] has been designed/developed to administer therapeutics to the upper part of the nasal cavity and to achieve a deposition of a larger fraction of pharmaceutics at the olfactory epihtelium compared with sprays, droppers, or pumps that usually deposit $< 5\%$ of the administered drug, thus ensuring a substantial level of drug delivery to the brain. A proof of concept study in humans has been successfully completed [20]. SipNose©'s nasal drug delivery devices utilize a novel mechanism ensuring accurate dose delivery, improved aerosol deposition at the olfactory epithelium, which in turn provides enhanced efficiency [115]. OptiNose© has performed a Phase I clinical trial to assess potential "nose-to-brain" oxytocin transport using its OptiNose Bi-Directional™ Breath Powered delivery platform. The OptiNose nasal delivery device which uses the natural function of the patient's breath to propel a pharmaceutic into the deep areas of the nasal cavity, permitted an efficient Nose-to-Brain oxytocin transport, while administering relatively low doses [116].

4.8. Drug delivery systems

Over the last decades, drug delivery systems have been established as a versatile platform for targeted drug delivery applications, as their unique features have been thoroughly investigated. Likewise to other administration pathways (e.g., oral, transdermal, etc.), formulation development approaches for nose-to-brain delivery applications have also attracted considerable interest and have so far demonstrated immense potential in providing protective and absorption-promoting effects to the encapsulated entities [6,7].

Various formulations have been utilized so far for CNS-targeted intranasal delivery applications, among which, micro- or nanoparticulate systems, micelles, solid lipid *nanoparticles* (SLNs), liposomes and emulsions have been the most extensively studied [7,117,118]. It has been shown that N2B drug transport aided by drug delivery systems can be achieved via various mechanisms (Table 2).

5. Nanocarrier mediated Nose-to-Brain delivery

The utilization of nanocarrier based formulations enhancing nasal absorption of pharmaceutics can be indicated as a promising approach for the enhancement of the efficacy of Nose-to-Brain delivery. This justifies the filing of patents on the development of appropriate formulations for N2B drug delivery (e.g., US7,989,502B2 [143] on intranasal delivery of modafinil, US9,375,400B2 [144] on manganese ion coated nanoparticles for delivery of compositions into the central nervous system by nasal insufflation). Both polymer and lipid-based formulations could facilitate drug transport through nasal mucosa while protecting their payload from enzymatic degradation and ensuring increased retention time at the mucosal surface, which can result to increased drug concentration at the site of interest [35,145]. Furthermore, the design of the nanocarriers can be tuned, regarding the selection of appropriate excipients, physicochemical properties (particle size distribution, zeta potential), biocompatibility/biodegradability, drug loading, spatial and temporal controlled drug release, etc [146]. Former review articles on Nose-to-Brain delivery of pharmaceutics, providing an excellent reference for previous work, have been published by Warnken et al. (2016), Lochhead (2012), Landis et al. (2012), Pardeshi and Belgamwar (2013), Dhuria et al. (2010), Mittal et al. (2014), and Samaridou and Alonso (2017) [7,9,16,25,29,41,147].

Table 3 reviews recent preclinical developments of various nanoparticulate drug delivery systems for Nose-to-Brain delivery.

5.1. Polymeric carriers

Nanoparticles based on both naturally derived polymers like chitosan and alginate, as well as synthetic polymers like polyesters (e.g., poly(lactide-*co*-glycolide), poly(lactic acid)) have been recently tested regarding their performance as Nose-to-Brain delivery systems (Table 3). The potential to select from a plethora of polymeric excipients and synthesis methods assists the fine-tuning of the formed nanocarriers with respect to morphological/molecular properties, drug encapsulation efficiency, drug release mechanism, targeting ability, bioresponsiveness, etc [174].

The FDA approved biocompatible and biodegradable polymers poly (lactide-co-glycolide) (PLGA) and poly(lactic acid) (PLA) with their

Table 2
Mechanisms of nanocarrier-aided drug transport.

Carrier	Transport mechanism
PLGA[a] NPs[b] [119]	• Transcellularly through olfactory axons
PEG[c]-PLA[d] NPs[b] [120]	• Transmucosal transport via the olfactory and trigeminal nerves pathways
CS[e]-NPs[b] [121]	• Clathrin dependent endocytosis (potential principal mechanism)
CS[e]-NPs[b] [122]	• Accumulation of NPs[b] in interstitial spaces. TQ[f] transport via opening of the tight junctions
CS[e], GCS[g], thiomer-based NPs[b] [123]	• Presence of DA[h] loaded GCS[g] NPs[b] in the right side of the olfactory bulb
Thiolated CS[e] NPs[b] [124]	• Paracellular transport
Thiolated CS[e] NPs[b] [125]	• Paracellular transport, inhibition of CYP450[i] enzyme
Mannitol-lecithin, CS[e] MPs[j] [126]	• Paracellular transport, insignificant axonal transport
DCH[k], MCD[l] MPs[j] [127]	• MCD[l] MPs[j]: Potentially, transport across the neuronal component of the olfactory mucosa
alginate NPs[b] [128]	• Mainly extracellular transport
PEG[c]-PCL[m] NPs[b] [129]	• Caveolae/clathrin-mediated endocytosis
poly(MMA-b-DMAEMA)[n]-functionalized PCL[m] NCs[o] [130]	• Mucoadhesion
TSP[p] MPs[j] [131]	• Mucoadhesive MPs with very similar structure with mucin
PS[q] NPs[b], CS[e] coated PS[q] NPs[b], polysorbate coated PS[q] NPs[b][16,132,133]	• NPs[b] transport was entirely transcellular (CS[e] coated PS[q] NPs[b] could allow transport of small MW[r] drugs paracellularly through the olfactory epithelium)
Micelles comprising Pluronic® L121 and P123 [134]	• Possible transcellular transport (sustentacular or neuronal cells)
Micelles comprising PEG-PCL[s] [135]	• Transport via the olfactory and trigeminal nerve
SLNs[t] [119]	• Transcellular transport through olfactory axons with diameter ~ 200 nm
SLNs[t], CS[e]-coated SLNs[t] [136]	• Mucoadhesion • Intracellular transport of [u]siRNA via olfactory and trigeminal nerve pathway
CS[e] coated NLC[v] [137]	• Transport through the olfactory and trigeminal nerve pathways
Nanocubic vesicles [138]	• Transcellular transport
Nanoemulsion, CS[e]-nanoemulsion [139]	• Mucoadhesion
Submicron emulsion [140]	• Increased ZT[w] permeation through nasal mucosa
Carbopol 934P-microemulsion [141]	• Increased tacrine transport through the nasal mucosa
CS[e]-NPs[b] and CS[e]-NPs[b] in a Pluronic F-127 gel [142]	• Very small CS[e]-NPs[b] can be transported through the axons and OB[x] to the olfactory cortex and to caudal pole of cerebral hemisphere and CL[y]
Nanoemulsion, CS[e]-nanoemulsion, nanoemulsion in a thermosensitive *in situ* forming gel [14]	• Drug transport via the maxillary nerve to the trigeminal nerve and olfactory nerve to the olfactory bulb and lastly to the brain

[a] Poly(lactic-co-glycolic acid).
[b] Nanoparticles.
[c] Poly(ethylene glycol).
[d] Poly(lactic acid).
[e] Chitosan.
[f] Thymoquinone.
[g] Glycol chitosan.
[h] Dopamine.
[i] Cytochrome P450.
[j] Microparticles.
[k] Chitosan chloride.
[l] Methyl-β-cyclodextrin.
[m] Poly(ε-caprolactone).
[n] Amphiphilic methacrylic copolymer constituted of methyl methacrylate and 2-(dimethylamino)ethyl methacrylate.
[o] Nanocapsules.
[p] Tamarind seed polysaccharide.
[q] Polystyrene.
[r] Molecular weight.
[s] Polyethylene glycol-polycaprolactone.
[t] Solid lipid nanoparticles.
[u] Small interfering RNA.
[v] Nanostructured lipid carrier.
[w] Zolmitriptan.
[x] Olfactory bulb.
[y] Cerebellum.

documented ability to achieve controlled drug release (e.g., sustained release up to several weeks or months), are the main synthetic polymers investigated for drug encapsulation [175]. PLGA and PLA NPs are generally synthesized via a double emulsion process where the polyester is dissolved in an appropriate solvent and the aqueous solution of the drug is emulsified with the aid of a sonicator into the PLGA solution followed by emulsification of the formed w/o emulsion in an aqueous solution of polyvinyl alcohol (PVA). Alternatively, PLGA NPs can be prepared by an o/w emulsification and nanoprecipitation process [175]. The incorporation of tarenflurbil (TFB) in PLGA NPs enhanced its delivery to the brain and resulted in increased absolute bioavailability of TFB following its intranasal administration to SD rats compared with intranasal administration of TFB solution and oral administration of TFB suspension [119]. Furthermore, the nasal delivery of lectin decorated, basic fibroblast growth factor (125I-bFGF) loaded pegylated PLGA (PLGA-PEG) nanoparticles to rats led to significantly increased presence of 125I-bFGF in the olfactory bulb (OB), cerebrum (CR), and cerebellum (CL) in comparison with intravenous delivery of the growth factor solution (Fig. 3). Increased concentration was also observed compared with nasal administration of 125I-bFGF solution and to a lesser extent compared with nasal delivery of unmodified 125I-bFGF loaded PLGA-PEG NPs [150]. Chitosan (CS) is a biocompatible, mucoadhesive cationic polysaccharide that comprises N-acetylglucosamine and D-glucosamine and is characterized by the unique

Table 3
Preclinical evaluation of nanocarriers for Nose-to-Brain delivery.

Carrier	Size (nm)	Zeta Potential (mV)	Drug/Disease	Drug Load. (wt%)/ Enc. Eff. (%)	PE[a]/TL[b]	Mode of admin.	Animal Model	% DTE[c]	% DTP[d]	Observations
Polymeric carriers										
PLGA[e] NPs[f] [119]	133.1	−30.2	TFB[g]/AD[h]	10/64.11	–	Instillation	SD[i] rats	287.24	65.18	Increased concentrations of TFB[g] in the brain compared to plasma concentrations 10 days after dose. Oral delivery of TFB[g] suspension and i.n.[j] delivery of TFB[g] solution failed to give similar results
PLGA[e] NPs[f] [148]	91.2	–23.7	OZ[k]/ schizo-phrenia	8.61/68.91	–	Instillation	White albino rats (250–300 g)	–	–	Enhanced brain concentration of OZ[k] and for a longer duration was observed in comparison with i.n.[j] and i.v.[l] delivery of OZ[k] solution
PEG[m]-PLGA[e] NPs[f] [149]	137.0	−30.0	coumarin-6	0.79/65.87	–/STL[n] (conj.eff. 79.52%)	Instillation	SD[i] rats	–	–	The presence of STL[n] increased targeting of various brain tissues. Enhanced dye concentration was observed in the OB[o], CR[p] and CL[q] compared with blood
PEG[m]-PLGA[e] NPs[f] [150]	118.7	−31.2	bFGF[r] /AD[h]	0.05/69.21	–/STL[n]	Instillation	Male SD[i] rats (200–230 g)	–	>70	STL[n] allowed efficient targeting of OB[o], CR[p] and CL[q]. Improvement of memory and spatial learning of AD[h] rats
PEG[m]-PLGA[e] NPs[f] [151]	114.8	–	UCN[s]/PD[t]	0.14/75.50	–/OL[u]	Instillation	Female mice (25–30 g) and female SD[i] rats (200–220 g)	–	–	Enhancement of the UCN[s] delivery to the brain and of neuroprotection of hemiparkinsonian rats
PEG[m]-PLA[v] NPs[f] [120]	110.8	2.4	coumarin-6	–	LMWP[w]/–	Instillation	Male SD[i] rats (200 ± 20 g)	–	–	LMWP[w] enhanced the presence of coumarin-6 in the CR[p], CL[q], OT[x] and OB[o] of the SD[i] rats Increased $AUC^{y}_{brain}/AUC^{y}_{blood}$ ratio was observed for the LMWP[w] functionalized NPs[f] implying enhanced nose-to-brain delivery
PEG[m]-PLA[v] NPs[f] [152]	100.0–1-20.0	–	^{125}I-VIP[z] (model neuroprotec-tive drug)	1.4/70.5	–/WGA[aa]	Instillation	Kunming mice (25–30 g), male SD[i] rats (230–280 g)	–	–	Enlarged AUC^{y} of intact VIP[z] in mice brain Improved spatial memory of rats.
PEG[m]-PLA[v] NPs[f] [153]	88.6–16-8.5	–	coumarin-6	4.0/50.0	–/UEA I[ab] (binds specifically to the olfactory epithelium)	Instillation	SD[i] rats (180–220 g)	–	–	Enhanced AUC^{y} of coumarin-6 in various brain tissues
CS[ac]-NPs[f] [121]	190.0	31.6	GH[ad]/AD[h]	9.86/23.34	–	Instillation (5mm inside the nostrils to allow reaching the olfactory epithelium)	Male Wistar rats (260–270 g)	–	–	Detection of NPs[f] in the OB[o], hippocampus, orbitofrontal and parietal cortices
CS[ac]-NPs[f] [154]	185.4–3-41.3	27.3 to 38.4	RHT[ae]/AD[h]	43.4–58.2 /75.1–85.3	–	Instillation	Wistar rats (4–5 months, 200–250 g)	355	71.80	High $AUC^{y}_{brain}/AUC^{y}_{blood}$ ratio, %DTE[c] and %DTP[d] indicating direct transport from nose to brain
CS[ac]-NPs[f] [155]	161.3	40.3	BRC[af]/PD[t]	37.8/84.2	–	Instillation	Swiss albino mice (20–40 g)	633	84.2	Increased nose to brain transport of BRC[af] loaded NPs[f] enhancing the drug's antioxidant effect At the same time, drug accumulation in GIT[ag] due to absorbtion via the systemic and/or nasopharynx pathways.
CS[ac]-NPs[f] [122]	150.0–2-00.0	–	TQ[ah]/AD[h]	31.2/63.3	–	Instillation	Male Wistar rats (5–6 months, 200–250 g)	3318.2-4	96.99	Enhancement of TQ[ah] brain transport
CS[ac]-NPs[f] [156]	269.0–3-82.0	–	ddI[ai]/HIV[aj]	9.1–47.3 / 90.7–94.6	–	Instillation	Male SD[i] rats (250–350 g)	–	–	Increased ddI[ai] concentration in CSF[ak], OB[o] and brain following i.n.[j] administration
CS[ac]-NPs[f] [157]	269.3	25.4	E2[al]/ AD[h]	–/64.7	–	Instillation		–	68.4	Direct rapid transport of E_2[al] to CSF[ak] following i.n.[j] administration

(*continued on next page*)

Table 3 (*continued*)

Carrier	Size (nm)	Zeta Potential (mV)	Drug/Disease	Drug Load. (wt%)/ Enc. Eff. (%)	PE[a]/TL[b]	Mode of admin.	Animal Model	% DTE[c]	% DTP[d]	Observations
							Male Wistar rats (250–300 g)			
CS[ac], GCS[am], thiomer-based NPs[f] [123]	214->1000	9.3 to 26.9	DA[an]/PD[t]	–/ up to 78.0	–	Instillation	Male Wistar rats (225–250 g)	–	–	Repetitive nasal administration of DA[an] loaded GCS[am] NPs[f] significantly enhanced the concentration of the neurotransmitter in the ipsilateral striatum
Thiolated CS[ac] NPs[f] [124]	272.1–2-82.9	20.9 to 27.7	CBZ[ao] /skeletal muscle conditions like pain and injury	5.4–6.1 /70.4–80.2	–	Instillation	Swiss albino mice (16–20 weeks, 20–25 g)	–	95.24—95.96	CS[ac] thiolation increased the brain uptake of CBZ[ao] and thus pain alleviation
Thiolated CS[ac] NPs[f] [125]	262.5	12.9	TZ[ap]/painful muscle spasms and spasticity	–/68.8	–	Instillation	Swiss albino mice (16–20 weeks, 20–25 g)	–	98.78—98.97	Increased mucosa permeation and brain uptake of TZ[ap] resulting in enhanced pain alleviation
N-TMC[aq] NPs[f] [158]	443.0	15.0	Leu-Enk[ar]/ analgetic	14.0/78.3	–	Instillation	Balb/c mice (20–25 g)	–	–	35-fold improved delivery of Leu-Enk[ar] compared to pure Leu-Enk[ar] solution and higher accumulation of fluorescent marker NBD-F[as] to the brain, which resulted into significant improvement in the antinociceptive effect of Leu-Enk[ar]
Mannitol-lecithin, CS[ac] MPs[at] [126]	2800.0, 2490.0		CPA[au]/brain injuries following stroke	9.7, 4.7/ 96.8, 94.6	–	Single dose Monopowder P® insufflator	Male Wistar rats (200–250 g)	–	–	Presence of CPA[au] in the CSF[ak] at increased concentration compared with blood Minimal amount of CPA[au] at the olfactory bulb
CG[av] MPs[at] [159]	1770.0—2210.0	–	RK[aw]/ *Acantha-moeba* systemic infections	13.7–14.2 /69.0–71.0	–	Single dose Monopowder P® insufflator	Male Wistar rats (200–250 g)	–	–	Presence of RK[aw] both in CSF[ak] and blood
DCH[ax], MCD[ay] MPs[at] [127]	1770.0, 3470.0	–	DFO[az]/	30.8/90.7, 31.7/95.1	–	Single dose Monopowder P® insufflator	Male Wistar rats (200–250 g)	–	–	DFO[az] was found in CSF[ak]
alginate NPs[f] [128]	173.7	37.40	VLF[aaa]/ depression	26.7/81.3	–	Instillation	Albino Wistar rats	425.8	76.5	Enhanced direct nose to brain delivery of VLF[aaa]. Improvement of behavioral analysis parameters and locomotor activity
PEG[m]-PCL[aab] NPs[f] [129]	88.4–89.-0	–23.6 to –23.1	NAP[aac]/AD[h]	0.6/47.6	–/Lf[aad]	Instillation	Male ICR mice (4–5 weeks, 20 ± 2 g) and male SD[i] rats (8–10 weeks, 220 ± 20 g)	–	–	Increased AUC[y] of coumarin-6 in various brain tissues Neuroprotection and memory improvement following intranasal administration of NAP[aac] loaded and Lf[aad] functionalized NPs[f] to mice
poly(MMA-b-DMAEMA)[aae] -functionalized PCL[aab] NCs[aaf] [130]	235.2–3-24.3	22.7 to 54.8	OLA[k]/ schizo-phrenia	–/99.0	–	Instillation	Male Wistar rats (200–250 g)	–	–	Increased uptake of OLA[k] in the brain; Improvement of prepulse inhibition impairment
TSP[aag] MPs[at] [131]	10,000	–	FITC-dextran	–	–	Nebulization	–	–	–	Increased deposition efficiency to the olfactory mucosa compared with MPs[at] of 2000 nm
PS[aah] NPs[f], CS[ac] coated PS[aah] NPs[f], polysorbate coated PS[aah] NPs[f] [17,132,133]	105.0–2-76.0	−42.1 to 30.1	–	–	–	Instillation	C57BL/ 6JBom male mice (~10 weeks, 20–25 g)	–	–	

(*continued on next page*)

Table 3 (*continued*)

Carrier	Size (nm)	Zeta Potential (mV)	Drug/Disease	Drug Load. (wt%)/ Enc. Eff. (%)	PE[a]/TL[b]	Mode of admin.	Animal Model	% DTE[c]	% DTP[d]	Observations
										NPs[f] could not be detected in the olfactory bulbs or cross the olfactory epithelium irrespectively of size, surface charge and surface modification CS[ac] coated PS[aah] NPs[f], were mainly found within the mucus layer, whereas some polysorbate coated PS[aah] NPs[f] could be seen in the olfactory epithelial cell layer, their number increasing with decreasing size. None of the NPs[f], were preferentially uptaken into olfactory axons over other epithelial cells possibly due to sizes > 100 nm
Micelles comprising Pluronic® L121 and P123 [134]	19.0–38-0.7	–	OLA[k]/ schizo-phrenia	0.5–1.8/ 10.3–75.0	–	Instillation	Male Wistar albino rats (200–250 g)	520.3	80.8	An important amount of OLA[k] could be detected in the brain
Micelles comprising PEG-PCL[aai] [135]	50.0–80.-0	positive	siRNA[aaj] or dextran as a model siRNA[aaj]	–	Tat-G[aak]/	Instillation	SD[i] male rats (8 weeks)			The functionalized micelles enabled mucosa permeation and siRNA[aaj] delivery to the brain
Lipid carriers										
SLNs[aal] [119]	169.9	−23.1	TFB[aam]/AD[h]	10.0/57.8	–	Instillation	SD[i] rats	183.1	45.4	Following i.n.[j] administration, TFB[aam] could be detected in the brain of rats even for reduced doses
SLNs[aal] [160]	148.0	−25.3	RSP[aan]	59.6/–	–	Instillation	Balb/C mice	–	–	Enhancement of RSP[aan] brain/blood ratio after i.n.[j] administration of RSP[aan] loaded SLNs[aal] in comparison with i.v.[i] administration
SLNs[aal], CS[ac]-coated SLNs[aal] [136]	335.8–4-69.7	-17.3 to 14.5	BACE1[aao] siRNA[aaj] /AD[h]	–	RVG-9R[aap] /	–	–	–	–	Enhanced permeation of siRNA[aaj] across epithelial cells
CS[ac] coated NLC[aaq] [137]	114.0	28.0	DiR[aar]	–	–	Instillation	Athymic nude female mice (22 g)			Effective delivery of the CS[ac] coated NLC[aaq] to the brain (CR[p], CL[q] and hippocampus) following i.n.[j] administration
GNLs[aas] [161]	172.0	−27.6	bFGF[aat]/PD[t]	4.6/86.7	–	Instillation	SD[i] rats	–	–	bFGF[aat] could be detected in the olfactory bulb and striatumtherapeutic effect was observed
Liposomes, [162]	178.9	−8.6	RHT[ae]/AD[h]	–/30.5	CPP[aau]	Instillation	Male SD[i] rats (200 ± 30 g)	–	–	CPP[aau] was found to enhance RHT[ae] delivery to the brain via both BBB[aav] permeation and olfactory route
Liposomes [163]	96.5	–	Fentanyl/ pain relief	~80/-	/RGD[aaw]	POD[aax] device[*]	Rats	–	–	Enhancement of analgesic effect and decrease of plasma fentanyl exposure
Transferomes [164]	310.0–8-85.0	–	OLA[k]/ schizo-phrenia	–/55.2–75.6	–	Instillation	Wistar albino rats (200–250 g)			Various values for brain $AUC^{y}_{0-360min}$ could be observed depending on the transferomes composition
Nanocubic vesicles [138]	363.0–6-45.0	–	OLA[k]/ schizo-phrenia	–/64.9–76.1	–	Instillation	Wistar albino rats (200–250 g)	100	–	Increased drug delivery to the brain
Emulsions										
Nanoemulsion [165]	144	−8.1	QTP[aay]/ schizo-phrenia	91% drug content		Instillation 10–15 mm into nasal cavity	Male Wistar albino rats (200–250 g)	267.9	63.6	Enhanced transport of QTP[aay] to the brain compared to pure QTP[aay] solution
Nanoemulsion [166]	176.3	−10.3	SQVM[aaz]/ neuro-AIDS	96.8	–	Instillation via a meter dose pump	Male SD[i] rats (250–270 g)	2919.3	96.6	Enhanced direct drug transport to the brain
Nanoemulsion, CS[ac]-nanoemulsion [139]	15.5, 16.7	−12.0, −9.1	RSP[aan]	99.1, 98.9	–	Instillation	Male Swiss albino rats (4–5 months, 200–250 g)	232.0, 476.0	57.0, 78.0	Increased brain/blood uptake ratio of RSP[aan] in the case of the mucoadhesive nanoemulsion signifying direct nose to brain transport
Nanoemulsion, CS[ac]-nanoemulsion [167]	20.1, 23.6	−8.4, −5.5	OLA[k]/ schizo-phrenia	99.0, 98.0	–	Instillation	Male Swiss albino rats (4–5 months, 200–250 g)	794.0, 890.0	87.0, 88.0	Increased brain/blood uptake ratio of OLA[k] in the case of the (mucoadhesive) nanoemulsion showing direct nose to brain transport

(*continued on next page*)

Table 3 (*continued*)

Carrier	Size (nm)	Zeta Potential (mV)	Drug/Disease	Drug Load. (wt%)/ Enc. Eff. (%)	PE[a]/TL[b]	Mode of admin.	Animal Model	% DTE[c]	% DTP[d]	Observations
Submicron emulsion [140]	153.5, 170.5	−31.4, 42.3	ZT[aba]/ migraine	/77.9 (in oil phase), 10.9 (in aqueous phase)	–	Instillation	Wistar rats	–	–	Increased AUC^{y}_{CSF}[ak]/AUC^{y}_{Plasma} in comparison with i.v.[l] administration The incorporation of the drug in the aqueous phase led to fast intranasal delivery of ZT[aba] both to blood circulation and brain
CS[ac]-microemulsion [168]	29.9–37.-1	10.8 to 13.7	Cab[abb]/PD[t], dementia, obesity	–	–	Instillation	Male Swiss albino rats (4–5 months, 150–200 g)	2766.7	94.3	CS[ac]-microemulsion successfully diffused through the nasal mucosa and exhibited enhanced brain uptake in comparison with intranasally administered microemulsion
Carbopol 940P-microemulsion [169]	19.9	−15.2	CZ[abc]/ epilepsy	–	–	Instillation	BALB/c mice (30–40 g)	–	91.2	Fast and efficient direct uptake of CZ[abc] in the brain
Carbopol 934P-microemulsion [141]	26.2	−34.3	Tacrine/AD[h]	98.9	–	Instillation	BALB/c mice (30–40 g), New Zealand rabbits (2.0–2.50 kg)	295.9	66.2	Enhanced direct nose-to-brain delivery of tacrine resulting in quick memory recovery in scopolamine-induced amnesic mice
Cs-Asp[abd]-HP-β-CD[abe]-microemulsion [170]	36.2	3.8	BH[abf] /anxiety	–/99.1	–		Wistar albino rats (180–220 g)	866.1	88.4	Direct nose-to-brain BH[abf] transport and significantly increased AUC^{y}_{0-360}min (brain) compared with i.v.[l] administration
Hybrid particles										
Lipid-PEG[m]-PLGA[e] NPs[f] [171]	153.6–1-75.5	−12.7 to −11.2	FTA[abg]/ glioblastoma	3.4–3.5/ 95.5–99.0	–	Instillation	Female Wistar rats (250–300 g)	–	–	Nasally administered FTA[abg] loaded NPs[f] permeated the mucus and could be found at high concentrations in the OB[o] and the brain in comparison with the i.v.[i] administered NPs[f] After 4 h
Inorganic particles										
MSNs[abh] [172]	263.5–2-83.5	−30.8 to −16.9	Curcumin, chrysin	11–14/–	–	Instillation	–	–	–	MSNs[abh] could be uptaken by the olfactory epithelial cells. pH dependent release of phytochemicals
Nanocarriers in thermoreversible gels										
CS[ac]-NPs[f] and CS[ac]-NPs[f] in a Pluronic F-127 gel [142]	164.5	28.3	Levodopa/ PD[t]	–/56.2	–	Instillation	Wistar rats	–	–	Maximum recovery of levodopa in brain was observed after i.n. of CS[ac]-NPs[f] in saline and not in the Pluronic F-127 gel due to limited availability of NPs[f] at the absorption membrane attributed to their slow migration from the gel
Microemulsion, mucoadhesive *in situ* gelling microemulsion [173]	150.0, 250.0	−15.0, −15.0	Nimodipine/ cerebrovas-cular spasm, dementia	70.0/–, 68.0/–	–	Instillation	male SD[i] rats (250–280 g)	–	–	The administration of the mucoadhesive *in situ* gelling microemulsion resulted in enhanced concentrations of nimodipine in brain and plasma
Nanoemulsion, CS[ac]-nanoemulsion, nanoemulsion in a thermosensitive *in situ* forming gel [14]	73.1–93-0.0, 108.5, 235.0	26, −1.2	DiR[aar], coumarin-6	–	–	Instillation	male SD[i] rats (200 ± 20 g)	–	–	Proof of concept for nanemulsion-aided direct nose to brain transport of drugs and of a minimum number of nanoemulsion droplets The droplet size, rather than the mucoadhesive coating or the impregnation in a thermosensitive *in situ* forming gel, mainly defines the in vivo fate of the nanoemulsion

[a] Permeation enhancer.
[b] Targeting ligand.
[c] Drug transport efficiency.
[d] Direct transport percentage.

[e] Poly(lactic-co-glycolic acid).
[f] Nanoparticles.
[g] Tarenflurbil.
[h] Alzheimer's disease.
[i] Sprague–Dawley.
[j] Intranasal.
[k] Olanzapine.
[l] Intravenous.
[m] Poly(ethylene glycol).
[n] Solanum tuberosum lectin.
[o] Olfactory bulb.
[p] Cerebrum.
[q] Cerebellum.
[r] Basic fibroblast growth factor.
[s] Urocortin peptide.
[t] Parkinson's disease.
[u] Odorranalectin.
[v] Poly(lactic acid).
[w] Low-molecular-weight protamine (as cell penetrating peptide).
[x] Olfactory tract.
[y] Area under the curve.
[z] Vasoactive intestinal peptide.
[aa] Wheat germ agglutinin.
[ab] Ulex europeus agglutinin I.
[ac] Chitosan.
[ad] Galantamine hydrobromide.
[ae] Rivastigmine.
[af] Bromocriptine.
[ag] Gastrointestinal tract.
[ah] Thymoquinone.
[ai] Didanosine.
[aj] Human immunodeficiency virus.
[ak] Cerebrospinal fluid.
[al] Estradiol.
[am] Glycol chitosan.
[an] Dopamine.
[ao] Cyclobenzaprine HCl.
[ap] Tizanidine HCl.
[aq] N-Trimethyl chitosan.
[ar] Leucine-enkephalin.
[as] 4-Fluoro-7-nitrobenzofurazan.
[at] Microparticles.
[au] N6-cyclopentyladenosine.
[av] Chitosan glutamate.
[aw] Rokitamycin
[ax] Chitosan chloride.
[ay] Methyl-β-cyclodextrin.
[az] Deferoxamine mesylate.
[aaa] Venlafaxine.
[aab] Poly(ε-caprolactone).

[aac] Neuroprotective peptide-NAPVSIPQ.
[aad] Lactoferrin.
[aae] Amphiphilic methacrylic copolymer constituted of methyl methacrylate and 2-(dimethylamino)ethyl methacrylate.
[aaf] Nanocapsules.
[aag] Tamarind seed polysaccharide.
[aah] Polystyrene.
[aai] Polyethylene glycole-polycaprolactone.
[aaj] Small interfering RNA
[aak] Cell penetrating peptide.
[aal] Solid lipid nanoparticles.
[aam] Tarenflurbil.
[aan] Risperidone.
[aao] β-secretase.
[aap] Cell penetrating peptide.
[aaq] Nanostructured lipid carrier.
[aar] Near infrared dye.
[aas] Gelatin nanostructured lipid carriers.
[aat] Basic fibroblast growth factor.
[aau] Cell penetrating peptide.
[aav] Blood brain barrier.
[aaw] Integrin targeting peptide.
[aax] Pressurized olfactory delivery.
[aay] Quetiapine.
[aaz] Saquinavir mesylate.
[aba] Zolmitriptan.
[abb] Cabergoline.
[abc] Clobazam.
[abd] Chitosan aspartate.
[abe] Hydroxypropyl-β-cyclodextrin.
[abf] Buspirone hydrochloride.
[abg] Farnesylthiosalicylic acid.
[abh] Mesoporous silica nanoparticles.
* Delivers aerosolized formulation preferentially to upper nasal cavity.

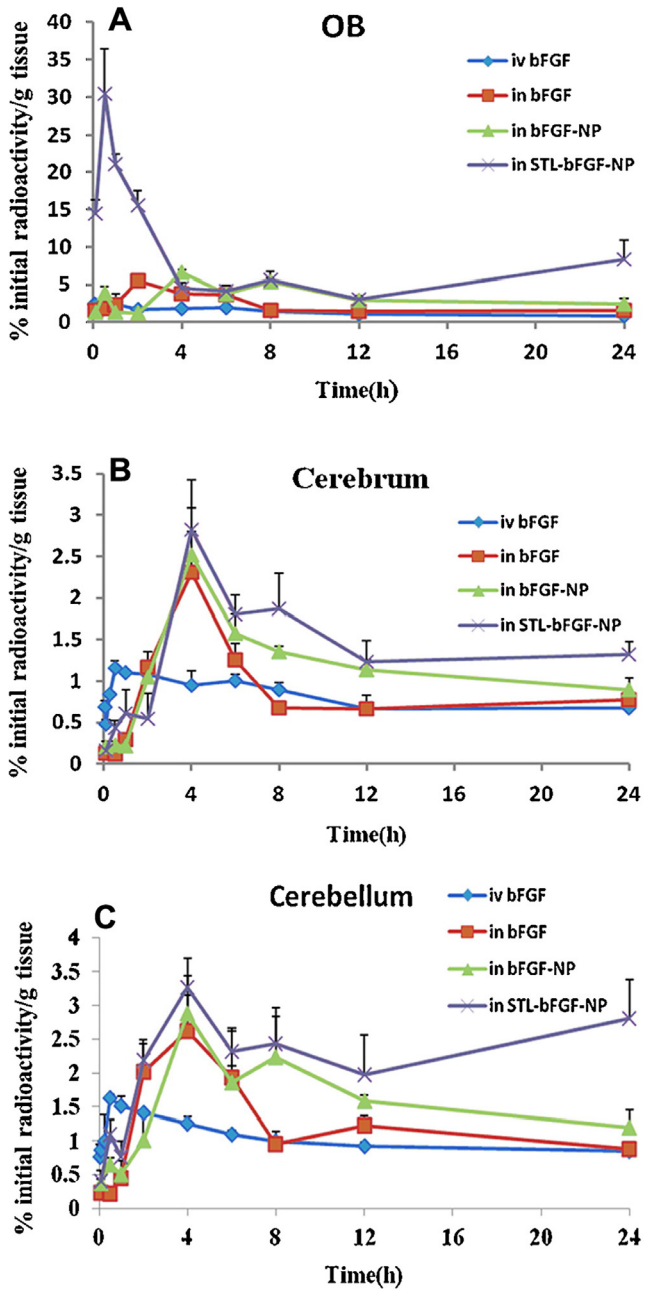

Fig. 3. Amount-time profiles of bFGF in the OB (A), CR (B), CL (C) following an intranasal administration of ^{125}I-bFGF solution, ^{125}I-bFGF-NP, STL-^{125}I-bFGF-NP and an intravenous injection of ^{125}I-bFGF solution. Data represented the mean ± S.E.M.(n = 4) [150].

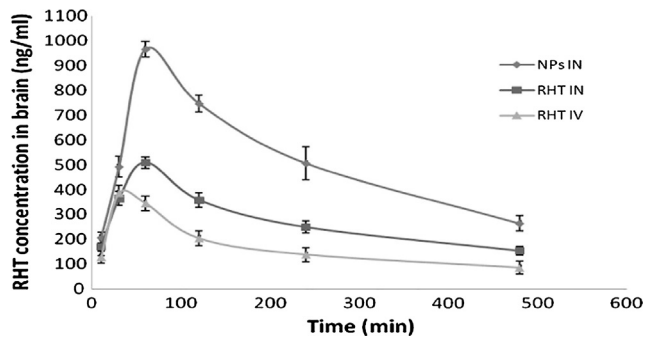

Fig. 4. Graph of RHT conc. in brain at different time intervals [154].

ability to facilitate the paracellular transport of biopharmaceuticals due to the transient opening of the tight junction structures [176,177]. (Thiolated) CS derivatives exhibiting increased mucoadhesion and/or enhanced permeation have been also synthesized [178]. Instant formation of CS particles can be achieved by ionic gelation with various polyanions (e.g., tripolyphosphate) [179–181]. The ionic complexation of galantamine hydrobromide (GH) with CS resulted in effective delivery of the neurotherapeutic drug to different sections of the brain following the instillation of the GH loaded CS NPs to the nostrils of rats [121]. Similarly, enhanced concentration of rivastigmine (RHT) was observed in the brain tissue, following its intranasal administration in the form of CS NPs formulation, in comparison with both intranasal and intravenous administration of RHT solution (Fig. 4) [154]. Additionally, thiolated CS NPs exhibited increased mucoadhesion and facilitated the direct nose-to-brain transport of the muscle relaxants cyclobenzaprine HCl (CBZ) and tizanidine HCl (TZ) while simultaneously minimizing cytotoxicity [124,125]. Poly (ε-caprolactone) (PCL) is an FDA approved, biodegradable, synthetic polyester. Drug-containing PCL particles are typically prepared by methods like solvent evaporation, solvent displacement, emulsion-solvent diffusion, etc [182]. Lactoferrin (Lf) modified PCL-PEG NPs enabled the effective biodistribution of coumarin-6 in various brain regions (e.g., OB, olfactory tract, hippocampus, CL and CB with hippocampus removed) of mice after the nasal administration of functionalized particle dispersions in comparison with non-functionalized NPs [129]. Haque and coworkers developed alginate NPs containing venlafaxine (VLF) which, following their intranasal administration to rats, exhibited improved brain/blood ratios for the administered drug in comparison with intranasal and intravenus administration of drug solutions [128]. *Polymer micelles* comprise another type of promising nanocarriers consisting of self-assembled amphiphilic block copolymers in an aqueous phase. They are characterized by small diameters (10–100 nm), flexibility regarding the control of their size and morphology via variation of the copolymer composition, block length ratios and molecular weight, as well as by the ability to incorporate hydrophobic drugs in their core and thus to protect them

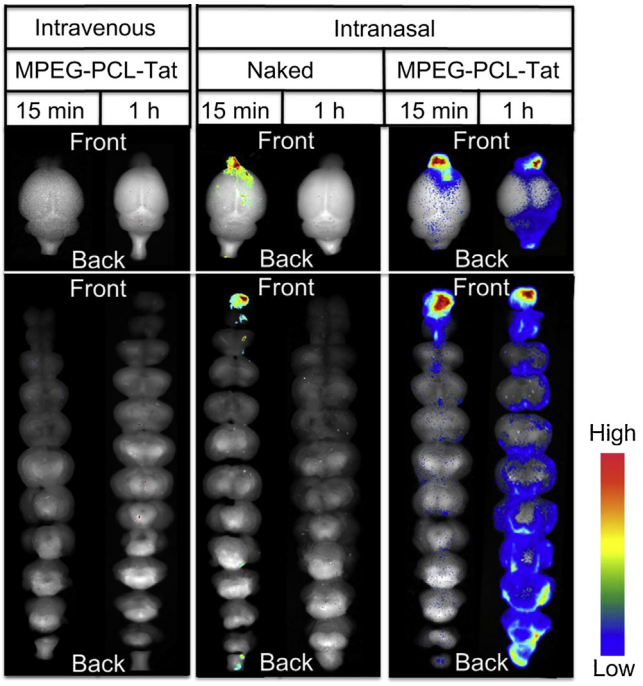

Fig. 5. Dynamics of MPEGePCLeTat complex in brain tissue following i.n. or i.v. administration. Rats were sacrificed and each brain was enucleated at each point after i.n. or i.v. administration of naked Alexa-dextran or Alexa-dextran/MPEGePCLeTat (dose ¼ 40 mg as Alexa-dextran). Each sample was observed using Maestro™ [135].

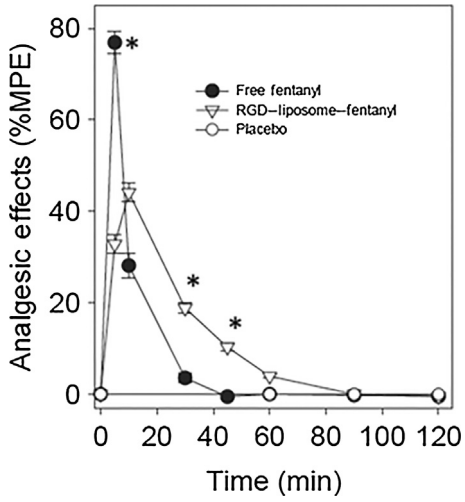

Fig. 6. Analgesic effect after nasal delivery of either free fentanyl or RGD liposome incorporated fentanyl. Rats were intranasally administered with 15 μg/kg fentanyl either in free and soluble (closed circles) or RGD liposome encapsulated form (open inverted triangle) while under isoflurane anesthesia. The tail flick test was performed over a 120 min period and analgesic effects were expressed as percentage MPE (or AUC_{effect}). The error bar indicates the SE of seven animals per group tested. Incorporating fentanyl into the RGD liposomes resulted in a lower analgesic effect at 5 min, significantly higher analgesic levels at 30 and 45 min, as well as a significantly higher AUC_{effect} ($^*p < 0.05$) [163].

from hydrolysis and enzymatic degradation, and their in vivo stability [183]. Kanazawa and coworkers, efficiently enhanced the nose-to-brain delivery of small interfering RNA (siRNA) via the development of polyethylene glycol-polycaprolactone (PEG-PCL) micelles containing dextran as a model siRNA and functionalized with a cell penetrating peptide derived from HIV-Tat. The functionalized nanocarriers exhibited enhanced mucosa permeability and enabled siRNA transport to the brain (Fig. 5) through the olfactory and trigeminal nerve pathways [135].

5.2. Lipid carriers

Solid lipid nanoparticles (SLNs), combining the advantages of liposomes and polymer NPs, consist of a biocompatible core of solid lipids, like triglycerides, enclosing the dissolved active pharmaceutical ingredient (mainly hydrophobic drugs and to a less extent hydrophilic macromolecules) and being stabilized by various surfactants [184–187]. It should be noted that the encapsulation of highly hydrophilic biomolecules into SLNs is relatively limited [186] resulting in the development of various methods potentially improving drug loading (e.g., high-pressure homogenization, solvent diffusion, double emulsion, etc) [188,189]. Rassu and coworkers effectively developed (CS-coated) SLNs for the Nose-to-Brain delivery of BACE1 (i.e., β-secretase 1) siRNA complexed with the glycoprotein derived peptide RVG-9R as a permeation enhancer to promote transport via the intracellular nerve pathway by receptor-mediated endocytosis. In vitro studies with epithelial cells monolayers confirmed the enhanced permeation of siRNA especially in the case of CS coated SLNs [136]. *Nanostructured lipid carriers (NLCs)* are colloidal structures comprising a lipid core composed of mixed solid and liquid lipids, responsible for the distinctive structures of the lipid matrix. NLCs can be considered advantageous to SLNs with respect to drug payload, storage stability, etc [184,190,191]. NLCs are typically prepared by the double emulsion (w/o/w) and the hot high-pressure homogenization methods [188]. NLCs with a CS coating exhibited increased residence time at the nasal epithelium and could be detected at various regions of the brain (e.g., CR, CL and hippocampus) after being intranasally administered at a single dose to mice without at the same time raising toxicity issues to the nasal mucosa [137]. *Liposomes* are concentric bilayered vesicles consisting of an aqueous core encompassed by numerous, few or just one phospholipid

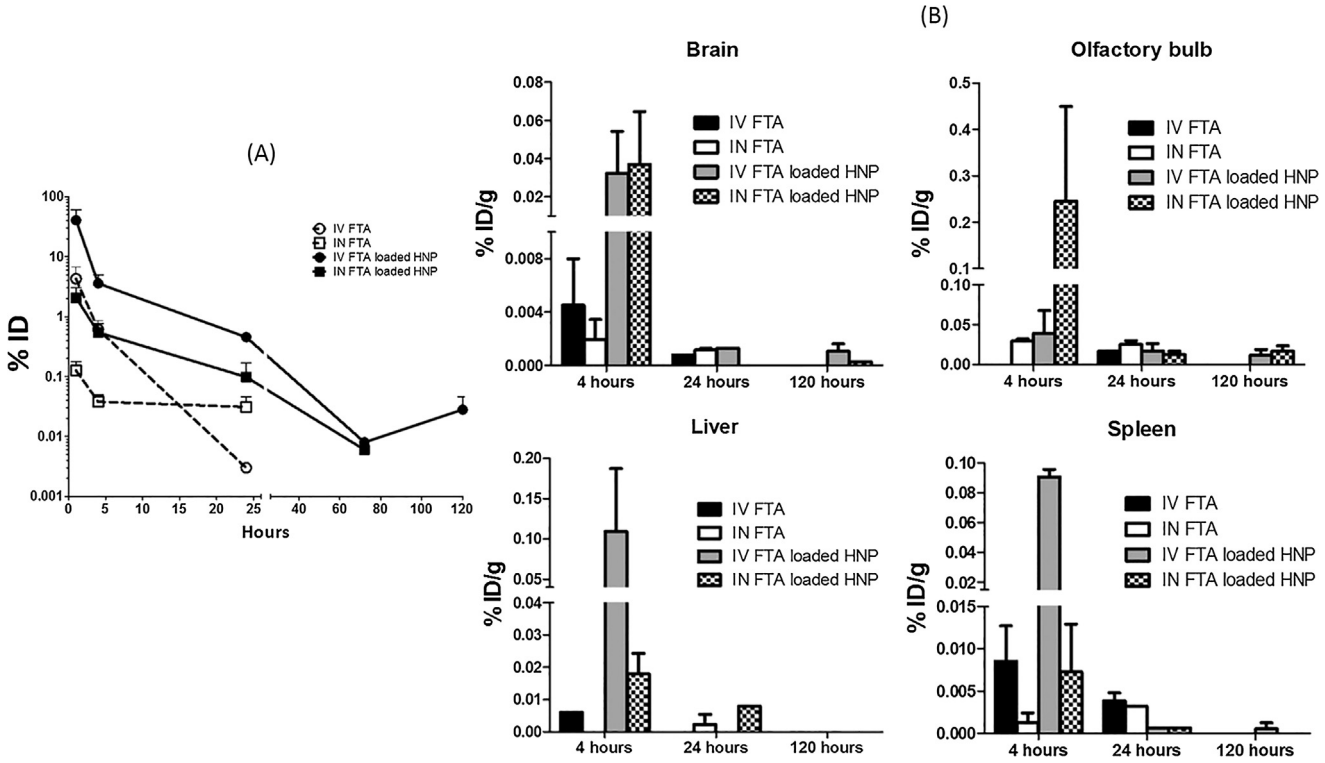

Fig. 7. Biodistribution study of the formulations in healthy rats. (A) Plasma FTA concentration versus time profile is represented for the treatment formulations. Data is shown a mean ± SEM, or as single point for n < 2. (B) The distribution of FTA in the brain, olfactory bulb, liver and spleen of healthy rats after 4, 24 and 120 h of formulation administration. Data is shown as mean ± SEM. Data with n < 2 are shown without error bars [171].

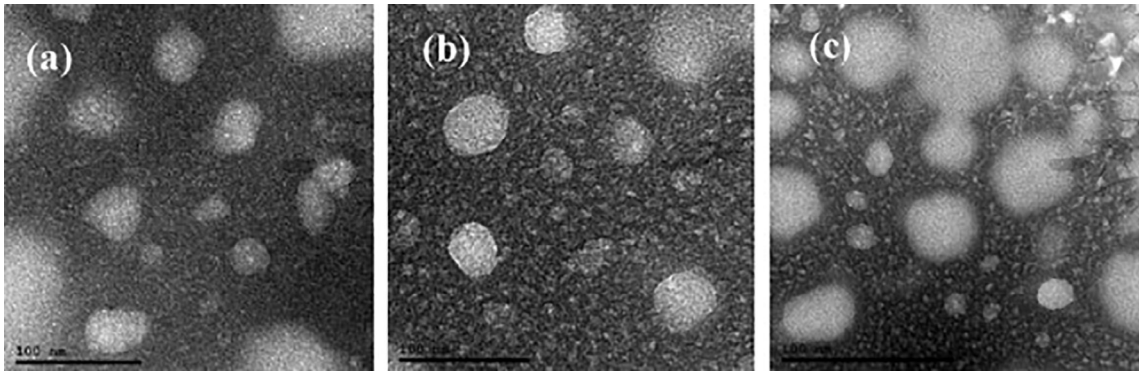

Fig. 8. TEM of buspirone hydrochloride microemulsion formulae (a) F1, (b) F2 and (c) F3 [170].

bilayers. They are typically prepared by the lipid film hydration-extrusion method and their morphology permits the incorporation of either hydrophilic or hydrophobic drugs in their inner aqueous phase or their lipid bilayer respectively. Moreover, being mainly based on naturally derived biodegradable excipients, liposomes can be considered innocuous [188,192]. Their efficiency as drug delivery systems has been proven by several marketed formulations as well as by promising clinical trial results [192]. Hoekman and coworkers developed fentanyl loaded liposomes functionalized with the integrin binding tripeptide Arg-Gly-Asp (RGD) targeting the nasal epithelium. When administered intranasally to rats with the aid of a pressurized olfactory drug delivery device (POD) which preferentially deposits the aerosol to the olfactory region of the nasal cavity, a long lasting analgesic effect was observed in compared to the administration of aerosolized drug, potentially attributed to a less rapid, sustained fentanyl release from the liposomal formulation (Fig. 6) [163].

In another study, hybrid NPs composed of a cationic lipid and PLGA-PEG were developed as nanocarriers for the intranasal and intravenous delivery of farnesylthiosalicylic acid (FTA) to glioblastoma. Biodistribution studies revealed the presence of the formulation in the brain following both i.n. and i.v. administration. However, a higher accumulation of NPs could be detected in the olfactory bulb post intranasal administration indicating direct Nose-to-Brain delivery via the olfactory pathway (Fig. 7) [171].

5.3. Emulsions

Emulsions (e.g., nanoemulsions, microemulsions) are considered an attractive type of nanocarriers due to their multiple advantageous characteristics, like increased biocompatibility as a consequence of their lipid constituents, resistance to enzymatic degradation, enhanced permeation through the epithelial mucosa, controlled release of APIs etc., and therefore are increasingly exploited by the pharma industry [184,193–195]. *Nanoemulsions* constitute isotropic nanodroplet dispersions of 20–500 nm [184,193,194,196], typically consisting of oil, surfactant and potentially a co-surfactant [196], which require increased energy input to form and are thermodynamically unstable. In contrast, *microemulsions* are thermodynamically stable, self-assembled systems comprising droplets (1–100 nm), spontaneously formed upon mixing an oil and aqueous phases and stabilized by appropriate surfactants [184,193,194,196]. Nanoemulsions can be optimized by associating a mucoadhesive excipient to prolong their residence time at the epithelium [197]. The intranasal administration of a saquinavir mesylate (SQVM) loaded nanoemulsion via a meter dose pump to rats resulted in enhanced SQVM concentration in the brain compared with the intravenous delivery of the drug suspension, thus entitling this formulation as promising for the delivery of anti-HIV medications to the CNS for the treatment of neuro-AIDS [166]. A CS coated, olanzapine (OLA) loaded nanoemulsion was also found to increase direct nose-to-brain transport of its cargo [167]. Sharma and coworkers developed a (CS coated) stable microemulsion for the efficient delivery of cabergoline (Cab), a potential medication for some neurological disorders, to the brain. The intranasal administration of the microemulsion with the mucoadhesive CS coating to rats led to direct Nose-to-Brain Cab transport and enhanced brain/blood uptake ratios, compared with the intranasal delivery of the Cab loaded microemulsion and the Cab solution as well as the intravenous administration of the drug-containing microemulsion [168]. Similar observations were presented by Florence and coworkers, who rapidly and effectively delivered clobazam (i.e., treating complex partial or acute seizures due to status epilepticus) to the brain via the intranasal administration route, in the form of a mucoadhesive (i.e., carbopol 940P coated) microemulsion [169]. In addition, Bshara, developed a mucoadhesive microemulsion, using chitosan aspartate, and hydroxypropyl-β-cyclodextrin, for the effective Nose-to-Brain delivery of buspirone hydrochloride (Fig. 8). Enhanced BH concentration levels in the brain and bioavailability were thus achieved [170].

5.4. Nanocarriers in thermoreversible gels

Thermoreversible gels have been already applied as formulations for the topical delivey of drugs (e.g., ocular, nasal administration). A widely used hydrophilic triblock copolymer, exhibiting temperature dependent phase transitions (e.g., from sol to gel and reverse) is poly (ethylene oxide-b-propylene oxide-b-ethylene oxide) known as Poloxamer 407 or Pluronic F127 (PF127) [142,198]. CS NPs containing levodopa (i.e., medication for Parkinson's disease) were intranasally administered to rats either incorporated in a PF127 based thermoreversible gel or in the form of a suspension. It was shown that even though the use of the hydrogel could prolong the residence of the formulation at the mucosa it could not facilitate the migration of the NPs towards the epithelium. Thus, the highest levodopa concentration in the brain was observed post intranasal administratin of the suspension of CS NPs followed by the application of a levodopa-loaded thermoreversible gel [142]. Additionally, Ahmad and coworkers assessed the efficiency of applying to the nose a thermosensitive gel (i.e., poloxamers 407 and 188) impregnated with a nanoemulsion, for Nose-to-Brain delivery, in comparison with the direct administration of the nanoemulsion and a mucoadhesive nanoemulsion (i.e., CS coated nanoemulsion). The study revealed that a small number of droplets can be delivered intact to the brain in contrast to their cargo (i.e., fluorescent dye) and it is the nanoemulsion droplet diameter that mainly contributes to the nanoemulsion fate post intranasal administration in comparison with the mucoadhesive coating or the gel impregnation [14].

5.5. Nanocarrier characteristics affecting Nose-to-Brain delivery

Little information is available about factors such as surface characteristics and size that may affect NPs transport from the nasal cavity

to the CNS. Due to the size of the tight junctions in the nasal cavity being in the order of 3.9–8.4 Å, and the suggestion that absorption enhancers can open the tight junctions only 10–15 times, it is likely that only NPs with a diameter less than 20 nm could achieve extracellular transport from the nasal cavity to the brain. Similarly, it is to be expected that only NPs with a diameter smaller than that of the olfactory axons (e.g., 100–200 nm in two month old rabbits and 100–700 nm in humans) can be intracellularly transported to the brain via the olfactory neural pathway [17]. In this respect, a study carried out with PS NPs and PS NPs modified either with chitosan (positive zeta potential) or polysorbate (negative zeta potential) with sizes in the range of 100–276 nm, indicated that the positively charged NPs were trapped in the mucus gel layer whereas a few of the negatively charged NPs could be detected in the olfactory epithelial cell layer but they were not uptaken into the olfactory axons. Furthermore, none of the NPs could be found in the olfactory bulb [17]. In another study by Ahmad and coworkers that focused on the tracking of nanoemulsion droplets and their cargo through the nose-to-brain pathway, it was demonstrated that the nanodroplets could be transported via the trigeminal and olfactory pathways to the olfactory bulb and finally to the brain, but in very small quantities. This phenomenon was pronounced for nanodroplets with diameters $\leq$100 nm that were less affected by mucociliary clearance. On the other hand, high amounts of their cargo were transported to the brain via the same pathways [13]. In general, cellular internalization of NPs is suggested to be dependent on concentration, particle size, surface charge and other surface characteristics such as lipophilicity [17]. The ubiquitous importance of the particle size can also be further ascertained by its direct correlation with the deposition patterns of particulate systems, as gravitational and sendimentation forces become determinants for particle sizes > 200 nm [62].

It should be mentioned at this point that although the particle size plays the most prominent role in the Nose-to-Brain transport of nanocarriers, other formulation parameters, such as the composition, type (polymer or lipid-based systems, particulates embedded in an *in situ* forming hydrogel, etc.) and surface characteristics, are all desicive in the determination of the fate of the formulation upon intranasal administration [62].

The values of the DTP% index and the physichochemical properties of the particulate systems as reported on Table 3 are plotted down in Fig. 9. Despite what was already mentioned previously regarding the effect of particle size, Fig. 9a fails to provide a direct correlation between the particle size and the DTP%. However, a more robust correlation between the surface charge and the DTP% could become evident in Fig. 9b. In particular, it can be observed that as the zeta potential approaches zero, higher DTP% values can be achieved.

Regarding the effect of the nanocarrier type (i.e., polymer NPs, liposomes, nanoemulsions, etc), on the Nose-to-Brain drug transport, this study showed that PLGA NPs (90–130 nm) [119,148] enhanced pharmaceutics concentration in the brain compared with intranasal delivery of drug solution, whereas the association of a targeting ligand to pegylated PLGA NPs (115–138 nm) [149–151] led to increased targeting of OB, CR and CC thus increasing drug delivery to the brain. Similarly, targeted PLA NPs [152,153] or PLA NPs bearing a permeation enhancer (89–168 nm) [120] increased the area under the curve (AUC) of drug in various brain tissues. CS NPs (150–382 nm) [121,122,154–157] were found to exhibit increased drug loading (e.g., up to 58.2 wt% [154]) and to exhibit increased nose-to-brain drug transport, possibly due to NPs mucoadhesion and drug transport through opening of tight junctions (paracellular transport). However, CS NPs of very small size could be also transported to various brain tissues via the axons. Chitosan thiolation was found to increase brain uptake again via paracellular transport [124,125]. It should be mentioned that a direct transport percentage (%DTP) up to ~ 99% was observed for tizanidine HCl (TZ) when administered intranasally with the aid of thiolated CS NPs [125]. Micelles were shown to facilitate transport through the olfactory and trigeminal nerves and thus siRNA delivery to the brain [135]. With respect to lipid-based nanocarriers, targeted liposomes (96.5 nm) effectively achieved drug transport to the brain [163], and SLNs (170 nm) permitted transcellular transport via the olfactory axons of Sprague-Dawley (SD) rats (~200 nm) and achieved drug delivery to the brain [119]. Furthermore, CS coated SLNs enabled siRNA transport through the trigeminal and olfactory nerves [136], whereas CS coated nanostructured lipid carriers (NLCs) of 114 nm could be detected in the brain (cerebrum (CR), cerebellum (CL) and hippocampus) following intranasal administration and transport through the trigeminal and olfactory nerve pathways [137]. In the case of nanoemulsions, enhanced brain/blood uptake ratios were observed also for mucoadhesive nanoemulsions (i.e., nanoemulsions associated with chitosan) achieving high %DTP (e.g., up to 96.6%) [166]. Similarly, rapid and efficient direct uptake of drugs in the brain could be succeeded using carbopol modified microemulsions [141,169], whereas a CS-modified microemulsion was shown to diffuse through the nasal mucosa and be uptaken in the brain [168]. Finally, the incorporation of nanocarriers in thermoreversible hydrogels allowed a longer residence of the formulation at the mucosa but at the same time impeded NPs migration to the epithelium [142].

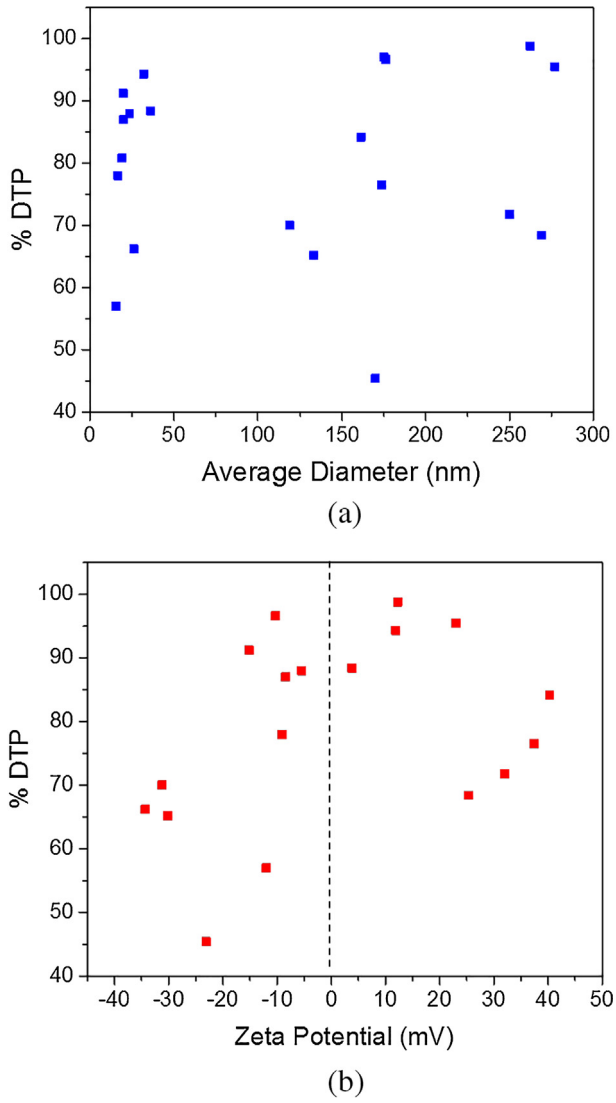

Fig. 9. Correlation between a) particle size and DTP% index and b) zeta potential and DTP% index.

6. In vitro and ex vivo models

In vitro (e.g., RPMI 2650 cells [199], olfactory mucosa primary cells [200]) and ex vivo (e.g., excised olfactory mucosa [6,132]) models have been used to study drug and/or nano- and microparticle permeability through the olfactory mucosa. With respect to in vitro models, Goncalves and coworkers examined the transport of a drug (i.e., ketoprofen) solution and drug loaded SLNs, NLCs and aerogel MPs through a multilayer of RPMI 2650 cells cultured in air-liquid interface. The cell multilayer exhibited comparable properties to excised nasal mucosa, regarding mucus production and transepithelial electrical resistance (TEER) values for sodium fluorescein. It was shown that, even though lacking ciliated cells and thus the possibility to simulate mucocilliary clearance, the in vitro model used was adequate for screening drug delivery formulations regarding their permeation through the nasal mucosa [199]. Additionally, Gartziandia and coworkers extracted primary cells from the olfactory mucosa of Wistar rats and developed an in vitro model based on an olfactory cell monolayer to examine the permeability of PLGA NPs and NLCs across this monolayer, thus simulating their permeability through the olfactory mucosa [200]. Regarding ex vivo models, the transport of polystyrene (PS) NPs of various sizes, and surface modified PS NPs, via the olfactory mucosa was assessed using a vertical Franz diffusion chamber where a freshly excised porcine olfactory epithelium was mounted. It was revealed that the NPs were associated with the olfactory mucus/epithelium but were not transported across the tissue [6,132].

7. Computational approaches

The computational investigation of drug delivery to the brain via the olfactory region has centered mainly on simulations of airflow during inhalation focusing on the motion of particles, gases, and droplets and their deposition onto the olfactory mucosa. Other aspects of the problem such as the interaction of deposited entities with the mucus layer, drug release, transfer through the mucus layer and the underlying epithelial layers have hardly been examined at all. There is an urgent need for computational models to describe these, to obtain a better understanding of the processes but also to assist in the design, execution, and analysis of existing and future experimental studies.

7.1. Delivery to the olfactory mucosa

The delivery of carrier particles and drugs to the olfactory mucosa through the nasal cavity is typically achieved by the use of inhaler devices either self-actuated (e.g., dry powder inhalers, DPIs) or assisted devices (e.g., metered dose inhalers, mDIs) and can be either in solid (e.g., DPIs) or in liquid (e.g., nasal sprays) form [201–203].

Predominantly, Computational Fluid Dynamics, CFD, has been used to determine the airflow in the nasal cavity and the transfer of molecules or particles to the olfactory region and deposition therein employing either approximate or realistic representations of the nasal geometry [204–207].

Computationally, the delivery of particles to the olfactory region is a challenging problem due to the highly curved nature of the nasal meatus folds within the nasal cavity, the dynamic nature of airflow, and the transitional nature, between laminar and turbulent, of airflow. Early computational grids for CFD simulations consisted of 1 m cells or less but accurate results require up to 10 m cells to properly describe the highly curved nature of the nasal cavity as well to resolve in detail the motion of particles near the nasal cavity surfaces [204]. The cross-sectional average Reynold numbers for flow through the nasal cavity vary with position and indicate laminar flow. However, due to the complex geometry, flow detachment can occur as well as formation and persistence of large eddies. Although, the transient effects indicated by the Womersley number seem borderline small, i.e., less than 1, they are magnified by the complex geometry of the nasal cavity. The airflow switches magnitude and direction every few seconds during an inhalation/exhalation cycle leading to an additional contribution to large eddy structures [204]. It should be noted that simulations in the olfactory cleft region indicate a recirculation flow, which can increase the residence time of particles and persists until the exhalation cycle, thus complicating flow simulations even more [208]. As a result, CFD simulations of nasal cavity airflow have been mostly conducted with either the k-ω SST RANS approach or Large Eddy Simulations, LES, which are very computationally expensive [204,205,209].

Particle or droplet transport can be modelled by including inertial forces, gravity, and diffusional motion [210]. A typical approach is to perform CFD simulations for a pure fluid (i.e., air) and then particles are "injected" into the air flow field and their trajectories are determined by solution of Newtons laws and taking into consideration the flow field determined by CFD. For the RANS approaches (e.g., k-ω, k-ε) airflow near the solid surfaces needs to be adequately resolved in order to obtain accurate near-wall particle trajectories which are necessary to determine collisions. The assumption of isotropic turbulence near the wall boundaries can also lead to errors and over-prediction of collision frequencies. Corrections can be introduced to properly determine the inertial terms, or more accurately, the transfer equations can be reformulated to include the local curvature of the wall boundary [211]. Particle motion due to turbulent dispersion is generally small for physiological flows and can be ignored as a first approximation but this does lead to small but systematic under-prediction of deposition rates.

Additional complications have to do with the dynamic nature of flow. Numerically, the flow field and particle motion have to be solved simultaneously leading to a significant increase in computational time [21]. Flow reversal also does not occur homogeneously and smoothly throughout the nasal cavity leading to more complicated flows in the olfactory cleft [204].

LES have been shown to generate improved results for particle deposition mostly due to the improved description of non-isotropy and turbulent dispersion. In steady flow simulations with LES, particle tracking can be performed based on an averaged LES flow field but the simulations still require significant computational [209].

To date computational simulations have revealed small deposition near the olfactory region varying with flow rate and particle size [206,207]. The largest percentage of deposition is observed with fine particles as larger particles are lost due to inertial impaction or by following the main airflow paths through the lower meatus air passages in the nasal cavity. For fine particles the deposition increases with decreasing particle size due to diffusional motion of the particles [206,207].

7.2. Carrier/mucosa interaction models

The carriers (i.e., liquid droplets or solid particles) interact in different ways with the olfactory mucus layer. Liquid droplets will spread to some degree while solid particles collide and generally adhere to the mucus layer. In the case of liquid droplets a drug transfer model is needed to describe the diffusion of drug to the mucus interface region, partitioning between liquid and mucus phases, and transfer to the mucus layer. Liquid droplets can spread, coalesce, or even detach from the mucus layer and mass transfer with the mucus layer can also occur. Therefore, liquid droplet spreading and stability models are needed.

Solid carrier particles can either transfer into the mucus layer or remain on the mucosa surface embedded in the mucus layer to some degree. Soft particles may deform and spread over the mucus layer. Mass transfer and drug release also occur after deposition. Several models are necessary to describe these interactions with the mucus layer. Mucoadhesion models are needed to describe attachment stability in terms of, electrostatic interactions, dispersion forces, hydrophobic interactions, chain interpenetration, etc. [212]. For soft solids spreading models are needed that account for the interfacial forces as well as the viscous, or viscoelastic, forces. Detailed particle models are

also required as particles can swell and erode either in a bulk or surface mode. In the case of hydrolysis degradation mechanisms surface erosion occurs in the limit of fast degradation kinetics and slow water uptake while bulk erosion occurs with slow degradation kinetics and fast water uptake [213,214]. However real systems are much more complicated and morphological changes can occur within the particle during erosion, influencing dramatically the rate of drug release.

The diffusion coefficient of the drug through the carrier particle can change with time and position due to swelling, degradation, and morphology changes. Different mass transfer pathways may become available including surface and bulk transfer through the pores [215]. Multipath diffusion models can be developed but these must take into account the varying morphology of the particles. Effective diffusion models can also be used but these need to determine the effective diffusion rate coefficient experimentally as a function of time and drug concentration.

The most important property of the carrier particles is the rate of drug release. Computational modelling of drug release from particles has been studied extensively for different environments, particles, and drugs. The rate of drug release needs to be quantified under different environments, which can differ significantly in terms of temperature, humidity, water content, hydrophobicity, ionic strength and can vary with time. Although there have not been many publications for drug release models in the olfactory region, there is a large body of work for pulmonary and intestinal mucosal environment [216].

Another important aspect of the drug release models is the initial drug profile in the carrier particle. The carrier drug might be distributed uniformly in the particle or may have a radial gradient or may have a significant proportion residing the carrier particle surface. The drug profile affects the release rate significantly. Surface-loaded drug molecules are released rapidly and this is observed as a “burst effect” in the literature [217]. The release rate from an inert carrier particle with an initial uniform profile decays exponentially due to the decrease in the particle drug load. Non-uniform drug profiles can result in different drug release rates.

Drug release models are always coupled to models describing the environment, e.g., mucus layer, and can also be strongly coupled to particle degradation or swelling models. The initial drug loading profile in the carrier particles, the particle model, and environment model (e.g., mucus layer) determine in a coupled manner the dynamic drug release rate.

7.3. Mucus layer penetration

Penetration through the mucus layer is achieved either by diffusion through the mucin fiber network or by surface diffusion via the paraneuronal pathway [9]. The transfer by diffusion of a drug or a drug-carrier entity, e.g., particle, liposome, through mucus layers is a very challenging problem that has only recently begun to be addressed by computational simulations [218,219].

The mucus layer environment is biologically complex (Section 2) with many entities dispersed within the mucin fibers including enzymes, lipids, macromolecules, macrophages, etc. The mucus layer is non-uniform, not only from a chemical perspective, but structurally as well. The mucin fiber network consists of mostly 100 nm network bridges but is traversed by porous passages that are many hundreds of nanometers in diameter. Drug molecules or particles can interact with the solvent, mucin chains, and other dispersed entities significantly affecting their transfer rate through the mucus layer.

Although computer simulations have been employed to investigate complex biological environments at a wide range of temporal and spatial scales the detail of biological systems that can be represented by computational simulations is necessarily limited by computational costs especially when describing interactions with particles and drug molecules up to time scales of milliseconds. Computational simulations of drug or particle transfer need to be conducted over a time period comparable to the characteristic time for diffusion which is on the order of microseconds for many drug molecules and milliseconds for nanoparticles, and simulations may have to account for drug/particle accumulation and degradation in the mucus layer or at the air mucus layer interface [220,221].

The mucus layer, being a complex heterogeneous and nonuniform system, is not easily described by full molecular dynamics, MD, simulations at the atomic level. However, some first attempts using coarse grained molecular dynamics, CGMD, have been recently presented for the mucus layer [222], as well as other complex biological barriers including the pulmonary surfactant layer [223], and other “crowded” biological environments, e.g., cytosol [224].

The CGMD simulations rely on a simplified system representation that describes a number of species but ignores the presence of other species in the mucus layer. The dispersed entities, e.g., drug molecule or nanoparticle as well as the entities of the biological environment, e.g., macromolecules and water molecules are represented in terms of coarse grained beads to simplify calculations. Coarse Graining, CG, is attractive for saving computational costs but presents significant trade-offs resulting in the inadequate description of some interactions and solvent effects. The CGMD approach can describe many processes, e.g., hydrodynamic interactions, electrostatic interactions, hydrophobic effects, volume restriction over time scales ranging from microseconds to milliseconds [224]. In CGMD different solvent simplifications are necessary depending on the interactions being modelled. [225].

Although Brownian and Stokesian dynamics can describe diffusion processes well they typically ignore intramolecular and conformation dynamics. More sophisticated physics-based CG models (e.g., PRIMO, OPEP, COFFDROP) combined with implicit solvent and/or models for hydrodynamic interactions are better suited for more detailed descriptions [224]. In CGMD approaches the choice of implicit or explicit solvent models and especially the water model is important.

In multiscale models, CG approaches can be combined with atomistic descriptions to provide a greater level of detail but additional challenges emerge, e.g., the appropriate integration of fine and coarse scale descriptions [225,226].

CG approaches can be applied to drug and particle transfer to examine the effect of properties (e.g., size, shape, surface properties), for various external flow fields (e.g., shear flow) and biological environments (e.g., mucus layers) on the motion, diffusion, and interaction with biological entities (e.g., macromolecules). Concerning the olfactory mucus layer, Wang and Shi [222] examined the diffusion of various nanoparticles through the mucus layer. They employed a CGMD approach based on regular and random networks of mucin fibers on the order of 50x50x50 nm computational cells and over a simulation time of 5 μs which is indicative of the current computational limitations of this approach. The authors employed bead representations of the fibrin fibers, nanoparticles, and water molecules (e.g., 9,216 polymer beads, 96,984 water beads) with different spring constants. They examined nanoparticles 2.1–4.6 nm in size as well as nanorods and observed indications of anomalous diffusion behavior (i.e., transition from normal to sub-diffusion for the larger particles). The diffusivity ratio with respect to water was found to vary strongly with particle size from 0.2 to 0.0006 for 2.1 to 4.6 nm particles, respectively. The authors also examined the effect of nanoparticle interactions with the mucin fibers by varying the interaction parameter of the Lennard Jones interaction potential and observed a decrease in the diffusivity due to transitional attachment to the mucin fiber network.

It is important to note that any particle traversing a biological barrier will not only interact with biological entities but also absorb them leading to the formation of a biological corona [227]. The biological corona in turn is what interacts with the biological environment and it is of dynamic nature, i.e., the corona thickness and composition changes depending on the biological environment. For example, in Hu et al. [223] the motion of 5 nm nanoparticles (1721 CG beads) through the pulmonary surfactant layer were examined by CGMD considering

both hydrophobic and electrostatic interactions for 90 nm polystyrene and hydroxyapatite nanoparticles. The authors found equilibrium position and translocation was most strongly determined by hydrophobic forces. Furthermore, the particles were coated by lipids and absorbed pulmonary surfactant to a degree that could influence the normal function of the surfactant layer [228]. Although electrostatic interactions were not found to be as significant as hydrophobic forces in the predominantly lipid environment of the pulmonary surfactant layer they should be a more significant factor in the more hydrophilic and charged environment of the mucus layer. Moreover, computational models for particles coated with a stabilizer layer need to describe the interaction of stabilizers with mucin chains during the particle transfer through the mucus layer [223].

In densely populated environments such as the cellular environment [224,229] there are crowding effects which have been found to have a significant effect on the diffusion properties and even biomolecular structure and activity [230]. Crowding effects are due to entropic excluded-volume effects but also additional factors such as hydrodynamic interactions [231]. Ando and Skolnick examined the crowding effect of macromolecules in the cellular environment with Stokesian Dynamics and found that excluded volume effects were significant resulting in a decrease in the diffusion coefficient by a factor of four in the cellular environment [232]. Solvation effects and compositional heterogeneity in the cytoplasm have also been examined [229]. The nasal mucus layers are approximated 5% solids providing a less crowded environment than in cells which have concentrations ranging from 100 to 450 g/L corresponding to 60–95% water. Also electrostatic forces should play a more important role in the mucus layer compared to the cytosol where the ionic strength is higher. Consequently, computational simulations of diffusion in the mucus layer may need to consider excluded volume effects and hydrodynamic interactions as these effects will be expected to lead to a decrease in the diffusion coefficient. In addition to these, electrostatic and hydrophobic interactions with respect to the mucin network also need to be described.

7.4. Epithelial layer transfer and physiologically based pharmacokinetic (PBPK) models

The drug or particle transfer rate through the mucus layer also depends on the transfer rate through the underlying epithelial layer as well as the clearance rate beyond the mucosal layer. There has been a significant body of work concerning transfer of molecules of different types and sizes as well as nanoparticles through epithelial and endothelial cells layers [233]. Computational studies on drug or nanoparticle transfer through epithelial layers are applicable to the olfactory submucosal epithelial cell layer with some key differences. For example transfer via the para-neuronal pathway is unique to the olfactory mucosa and the clearance pathways past the epithelial cell layers are considerably different. Experimental studies do indicate different transfer pathways (e.g., paracellular, transcellular) depending on the size and nature of the drug [9].

Note that particle transiting the mucus layer will be surrounded by a biological corona that will influence not only the transfer through the mucus layer but also through the epithelial layer [223,228]. NPs will form a corona removing macromolecules and enzymes from the mucus layer and may change the composition of the mucus layer perhaps even the structure of as many of the mucus fibrin entanglements are reversible.

Also of interest is the possibility of disruption of both the mucus layers and the epithelial layers due to the passage of NPs. Simulations have also indicated temporary disruption of the membrane due to the passage of a NP even with formation of holes [234].

Finally, NP passage through the epithelial layer can be incomplete, as particles can become trapped in the membrane or in the cytosol or some cellular compartments e.g. lysosome [219].

Physiologically based pharmacokinetic (PBPK) modeling has developed rapidly within the pharmaceutical industry and is becoming an integral part of drug development [235]. PBPK modelling of drug delivery through to the respiratory system requires a description of drug transfer at the target sites, e.g., alveoli, respiratory mucosa, nasal mucosa [236]. Nasal drug transfer requires a description of carrier deposition, drug release, and absorption/penetration at the target regions of the nasal cavity, e.g., olfactory mucosa, cells. The description of drug inflow to the PBPK models needs to be integrated with other models, e.g., particle flow and deposition, drug release, mucous penetration [236]. This integration is challenging but can improve the accuracy and broaden the predictions of PBPK models. For example, Vulovic et al. (2018) combined CFD with PBPK modeling in order to predict aerolisolization of different dry powder formulations and estimate in vivo deposition and absorption of amiloride hydrochloride in the pulmonary region [237].

7.5. Interface computational models

Although highly advantageous due to its non-invasive nature, rapid onset of action and highly localized delivery resulting in low systemic exposure, the delivery of medications to the brain via the nasal cavity exhibits particular challenges, associated with poor permeability across biological barriers (e.g., nasal and olfactory mucosae) and poor stability attributed to enzymatic activity observed in the nasal cavity. The European H2020 Research and Innovation Project "*Nose to Brain Delivery of NG-101 via the Olfactory Region for the Regenerative Treatment of Multiple Sclerosis Using Novel Multifunctional Biomaterials Combined with a Medical Device, N2B-patch*" focuses on the development of a novel galenic formulation based on multifunctional biomaterials for the continuous release of biopharmaceutics at the olfactory mucosa. This formulation will consist of biodegradable particles containing a therapeutic biomolecule, incorporated in a biodegradable hydrogel that will be deposited onto the olfactory epithelium with the aid of an

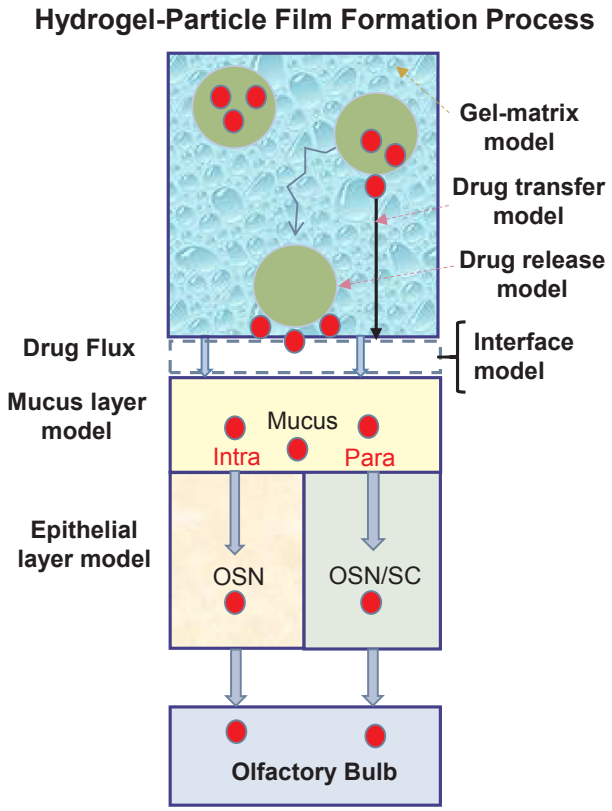

Fig. 10. Modeling of drug transport from the embedded particles to the olfactory bulb (OSN: olfactory sensory neurons, SC: Support cells).

Table 4
Computational models that will predict the overall performance of the developed N2B formulation.

Sub-Models	Characteristic Times
• Modeling of hydrogel i) extrusion from the applicator, ii) mucoadhesion and film formation on the olfactory epithelium, and iii) stability/detachment	• Hydrogel film formation time ($t_{m,form}$) • Hydrogel degradation time ($t_{m,deg}$)
• Mathematical models for biomolecule release rate from the embedded particles and particle degradation, in terms of particle morphological and molecular properties as well as environmental conditions	• Particle degradation time ($t_{p,deg}$) • Drug diffusion time ($t_{d,diff}$)
• Hydrogel model: degradation, swelling, transport of particles and therapeutic biomolecule across the hydrogel film	• Hydrogel degradation time ($t_{m,deg}$)
• Integrated model	• Drug accumulation time ($t_{d,acc}$)

endoscopic applicator.

The computational models described in 6.1–6.4 are connected at the interface layer separating the hydrogel matrix and the olfactory mucosal surface. Interactions (e.g., mass transfer, adhesion, interpenetration, and transfer) between particles, drug, and hydrogel matrix and the mucus layer need to be described by experimental and computational approaches. Fig. 10 shows the interface computational models that will be developed in the framework of this project to predict the overall performance of the aforementioned N2B formulation. The mathematical models (described in Table 4) aim to connect the main drug flux processes from the particles incorporated in the hydrogel to the mucus gel layer and subsequently through the olfactory epithelium to the olfactory bulb.

8. Conclusions

Different types of nanocarriers (e.g., polymer or lipid-based) were shown to facilitate the Nose-to-Brain delivery of their cargo, for example by adhering to the olfactory epithelium (mucoadhesion and/or targeting) and allowing the paracellular or intracellular transport of the drug, whereas in rare cases direct transport of the nanocarriers (usually of average sizes ≤ 200 nm) could be achieved via the olfactory and trigeminal nerve pathways. According to the above, the nanocarriers should have small size (preferentially below 100 nm) to ensure that they will not be strongly affected by mucocilliary clearance and that they could be transported via the olfactory and trigeminal nerve pathways. At the same time, the nanocarriers should exhibit mucoadhesive properties to increase their residence time at the olfactory mucosa and also exhibit increased drug loading to ensure a lower dosage form. To date no solid evidence has been provided confirming nose-to-brain transport of intact nanocarriers, which on the other hand could be considered beneficial since the accumulation of excipients in the brain might result in undesirable side effects. A systematic investigation of both lipid and polymer-based formulations and their application in nasal delivery could aid towards realistically evaluating their potential for direct nose-to-brain transport and reveal both their strengths and weaknesses.

The total dose delivered to the target region is the key endpoint for effective pharmaceutical action. The total dose depends on the total amount of drug transferred through the olfactory mucosa but it also depends on the transfer and distribution within the brain which is known to be both dynamic and strongly non-uniform. The bio-distribution of drug within the brain and its relation to effective dose will be a key area of research in the immediate future.

Regarding computational modelling, it has focused so far on targeting of the olfactory region during inhalation. Research into drug, particle, and droplet interaction with, as well as transfer through the olfactory mucus layer is still at an early stage but is expected to progress rapidly in the coming decade.

Acknowledgments

The present research has been financially supported by EU under the European Framework Programme for Research and Innovation Horizon 2020 (Grant No. 721098).

References

[1] M. Simonato, J. Bennett, N.M. Boulis, M.G. Castro, D.J. Fink, W.F. Goins, S.J. Gray, P.R. Lowenstein, L.H. Vandenberghe, T.J. Wilson, J.H. Wolfe, J.C. Glorioso, Progress in gene therapy for neurological disorders, Nat. Rev. Neurol. 9 (2013) 277–291.
[2] X. Xu, A.E. Warrington, A.J. Bieber, M. Rodriguez, Enhancing central nervous system repair - The challenges, CNS Drugs. 25 (2011) 555–573, http://dx.doi.org/10.2165/11587830-000000000-00000.
[3] P. Sweeney, H. Park, M. Baumann, J. Dunlop, J. Frydman, R. Kopito, A. McCampbell, G. Leblanc, A. Venkateswaran, A. Nurmi, R. Hodgson, Protein misfolding in neurodegenerative diseases: implications and strategies, Transl. Neurodegener. 6 (2017).
[4] R.R. Ramsay, M. Majekova, M. Medina, M. Valoti, Key targets for multi-target ligands designed to combat neurodegeneration, Front. Neurosci. 10 (2016).
[5] L. Kozlovskaya, M. Abou-Kaoud, D. Stepensky, Quantitative analysis of drug delivery to the brain via nasal route, J. Control. Release. 189 (2014) 133–140.
[6] L. Illum, A. Mistry, S. Stolnik, Nanoparticles for direct nose-to-brain delivery of drugs, Int. J. Pharm. 379 (2009) 146–157.
[7] Z.N. Warnken, H.D.C. Smyth, A.B. Watts, S. Weitman, J.G. Kuhn, R.O. Williams, Formulation and device design to increase nose to brain drug delivery, J. Drug Deliv. Sci. Technol. 35 (2016) 213–222.
[8] B. Engelhardt, L. Sorokin, The blood-brain and the blood-cerebrospinal fluid barriers: function and dysfunction, Semin. Immunopathol. 31 (2009) 497–511.
[9] J.J. Lochhead, R.G. Thorne, Intranasal delivery of biologics to the central nervous system, Adv. Drug Deliv. Rev. 64 (2012) 614–628.
[10] L. Illum, Is nose-to-brain transport of drugs in man a reality? J. Pharm. Pharmacol. 56 (2004) 3–17.
[11] J.J. Lochhead, D.J. Wolak, M.E. Pizzo, R.G. Thorne, Rapid transport within cerebral perivascular spaces underlies widespread tracer distribution in the brain after intranasal administration, J. Cerebral Blood Flow Metab. 35 (2015) 371–381.
[12] E. Yuba, K. Kono, Nasal Delivery of Biopharmaceuticals, in: J. das Neves, B. Sarmento (Eds.), Mucosal Deliv. Biopharm., Springer US, Boston, MA, 2014: pp. 197–220.
[13] H. Chen, G.Z.X. Yang, H. Getachew, C. Acosta, C. Sierra Sánchez, E.E. Konofagou, Focused ultrasound-enhanced intranasal brain delivery of brain-derived neurotrophic factor, Sci. Rep. 6 (2016) 28599.
[14] E. Ahmad, Y. Feng, J. Qi, W. Fan, Y. Ma, H. He, F. Xia, X. Dong, W. Zhao, Y. Lu, W. Wu, Evidence of nose-to-brain delivery of nanoemulsions: cargoes but not vehicles, Nanoscale 9 (2017) 1174–1183.
[15] J. Stevens, B.A. Ploeger, P.H. van der Graaf, M. Danhof, E.C.M. de Lange, Systemic and direct nose-to-brain transport pharmacokinetic model for remoxipride after intravenous and intranasal administration, Drug Metab. Dispos. 39 (2011) 2275–2282.
[16] M.S. Landis, T. Boyden, S. Pegg, Nasal-to-CNS drug delivery: where are we now and where are we heading? An industrial perspective, Ther. Deliv. 3 (2012) 195–208.
[17] A. Mistry, S. Stolnik, L. Illum, Nose-to-brain delivery: Investigation of the transport of nanoparticles with different surface characteristics and sizes in excised porcine olfactory epithelium, Mol. Pharm. 12 (2015) 2755–2766.
[18] M. Stützle, J. Flamm, S. Carle, K. Schindowski, Nose-to-brain delivery of insulin for Alzheimer's disease, Admet Dmpk. 3 (2015) 190–202.
[19] D.S. Quintana, L.T. Westlye, O.G. Rustan, N. Tesli, C.L. Poppy, H. Smevik, M. Tesli, M. Røine, R.A. Mahmoud, K.T. Smerud, P.G. Djupesland, O.A. Andreassen, Low-dose oxytocin delivered intranasally with Breath Powered device affects social-cognitive behavior: A randomized fourway crossover trial with nasal cavity dimension assessment, Transl. Psychiatry. 5 (2015).
[20] Impel Neuropharma Inc., POD Technology, (2017). http://impelnp.com/pod-technology.
[21] P. Karakosta, A.H. Alexopoulos, C. Kiparissides, Computational model of particle deposition in the nasal cavity under steady and dynamic flow, Comput. Methods Biomech. Biomed. Engin. 18 (2013) 514–526.
[22] S. Gizurarson, Anatomical and histological factors affecting intranasal drug and vaccine delivery, Curr. Drug Deliv. 9 (2012) 566–582.
[23] L. Illum, Potential for nose-to-brain delivery of drugs, in: A. Tsuda, P. Gehr (Eds.), Nanoparticles Lung - Environ, CRC Press, Expo. Drug Deliv., 2014, pp. 1–368.
[24] J.R. Harkema, S.A. Carey, J.G. Wagner, The nose revisited: A brief review of the

comparative structure, function, and toxicologic pathology of the nasal epithelium, Toxicol. Pathol. 34 (2006) 252–269.
[25] C.V. Pardeshi, V.S. Belgamwar, Direct nose to brain drug delivery via integrated nerve pathways bypassing the blood-brain barrier: an excellent platform for brain targeting, Expert Opin. Drug Deliv. 10 (2013) 957–972.
[26] L. Illum, Transport of drugs from the nasal cavity to the central nervous system, Eur. J. Pharm. Sci. 11 (2000) 1–18.
[27] C. Bitter, K. Suter-Zimmermann, C. Surber, Nasal drug delivery in humans, in: C. Surber, P. Elsner (Eds.), Top, Appl. Mucosa, KARGER, Basel, 2011, pp. 20–35.
[28] P.G. Djupesland, J.C. Messina, R.A. Mahhoud, The nasal approach to delivering treatment for brain diseases: an anatomic, physiologic, and delivery technology overview, Ther. Deliv. 5 (2014) 709–733.
[29] S.V. Dhuria, L.R. Hanson, W.H. Frey, Intranasal delivery to the central nervous system: Mechanisms and experimental considerations, J. Pharm. Sci. 99 (2010) 1654–1673.
[30] M.I. Ugwoke, R.U. Agu, N. Verbeke, K. Renaat, Nasal mucoadhesive drug delivery: Background, applications, trends and future perspectives, Adv. Drug Deliv. Rev. 57 (2005) 1640–1665.
[31] R.A. Cone, Barrier properties of mucus, Adv. Drug Deliv. Rev. 61 (2009) 75–85.
[32] E.R. Lillehoj, K.C. Kim, Airway mucus: Its components and function, Arch. Pharm. Res. 25 (2002) 770–780.
[33] S. Girod, J.-M. Zahm, C. Plotkowski, G. Beck, E. Puchelle, Role of the physiochemical properties of mucus in the protection of the respiratory epithelium, Eur. Respir. J. 5 (1992) 477–487.
[34] M. King, Mucus and its role in airway clearance and cytoprotection, in: Q. Hamid, J. Martin, J. Shannon (Eds.), Physiol, Basis Respir. Dis, BC Decker, 2005, pp. 409–416.
[35] Y. Ozsoy, S. Gungor, E. Cevher, Nasal delivery of high molecular weight drugs, Molecules. 14 (2009) 3754–3779.
[36] D. Fitzpatrick, The chemical senses, in: D. Purves, G.J. Augustine, D. Fitzpatrick, W.C. Hall, A.S. LaMantia, J.O. McNamara, S.M. Williams (Eds.), Neuroscience, 3rd Editio, Sinauer Associates Inc, Sunderland (MA), 2003.
[37] B.P.M. Menco, Ciliated and microvillous structures of rat olfactory and nasal respiratory epithelia - A study using ultra-rapid cryo-fixation followed by freeze-substitution or freeze-etching, Cell Tissue Res. 235 (1984) 225–241.
[38] E. Meisami, J. Louie, R. Hudson, H. Distel, A morphometric comparison of the olfactory epithelium of newborn and weanling rabbits, Cell Tissue Res. 262 (1990) 89–97.
[39] M.J. Lawson, B.A. Craven, E.G. Paterson, G.S. Settles, A computational study of odorant transport and deposition in the canine nasal cavity: Implications for olfaction, Chem. Senses. 37 (2012) 553–566.
[40] H. Lenz, Die Oberfläche Der Regio Olfactoria Des Menschen IM Rasterelektronenmikroskop, Acta Otolaryngol. 84 (1977) 145–154.
[41] D. Mittal, A. Ali, S. Md, S. Baboota, J.K. Sahni, J. Ali, Insights into direct nose to brain delivery: current status and future perspective, Drug Deliv. 21 (2014) 75–86.
[42] W.A. Banks, Delivery of peptides to the brain: Emphasis on therapeutic development, Biopolym. - Pept. Sci. Sect. 90 (2008) 589–594.
[43] W.A. Banks, Characteristics of compounds that cross the blood-brain barrier, BMC Neurol. 9 (2009) S3.
[44] J. Skipor, B. Wasowska, W. Grzegorzewski, A. Zezula-Szpyra, S. Stefanczyk-Krzymowska, J.-C. Thiéry, Transfer of dopamine by counter-current mechanism in the ewe changes with endocrine stage, Biog. Amin. 16 (2001) 431–445.
[45] J. Muszak, T. Krzymowski, P. Gilun, S. Stefanczyk-Krzymowska, Countercurrent transfer of dopamine from venous blood in the cavernous sinus to the arterial blood supplying the brain - Tlhe perfused rabbit head as an experimental model, J. Physiol. Pharmacol. 65 (2014) 641–648.
[46] N. Einer-Jensen, L. Larsen, Local transfer of diazepam, but not of cocaine, from the nasal cavities to the brain arterial blood in rats, Pharmacol. Toxicol. 87 (2000) 276–278. papers2://publication/uuid/8EADC72D-EC5C-4D0E-96BA-2BFEB365D749.
[47] N. Einer-Jensen, L. Larsen, Transfer of tritiated water, tyrosine, and propanol from the nasal cavity to cranial arterial blood in rats, Exp. Brain Res. 130 (2000) 216–220.
[48] W. Grzegorzewski, J. Skipor, B. Wasowska, T. Krzymowski, Counter current transfer of oxytocin from the venous blood of the perihypophyseal cavernous sinus to the arterial blood of carotid rete supplying the hypophysis and brain depends on the phase of the estrous cycle in pigs, Biol. Reprod. 52 (1995) 139–144.
[49] W.M. Pardridge, Drug transport in brain via the cerebrospinal fluid, Fluids Barriers CNS. 8 (2011).
[50] S.V. Dhuria, L.R. Hanson, W.H. Frey, Novel vasoconstrictor formulation to enhance intranasal targeting of neuropeptide therapeutics to the central nervous system, J. Pharmacol. Exp. Ther. 328 (2009) 312–320.
[51] M. Dahlin, Nasal administration of compounds active in the Central Nervous System - Exploring the olfactory pathway, Uppsala University, Ph.D Dissertation, (2000).
[52] R.G. Thorne, W.H. Frey, Delivery of Neurotrophic Factors to the Central Nervous System, Clin. Pharmacokinet. 40 (2001) 907–946.
[53] E.E. Morrison, R.M. Costanzo, Morphology of olfactory epithelium in humans and other vertebrates, Microsc. Res. Tech. 23 (1992) 49–61.
[54] K. Buchner, D. Seitz-Tutter, K. Schönitzer, D.G. Weiss, A quantitative study of anterograde and retrograde axonal transport of exogenous proteins in olfactory nerve C-fibers, Neuroscience. 22 (1987) 697–707.
[55] K. Kristensson, Y. Olsson, Uptake of exogenous proteins in mouse olfactory cells, Acta Neuropathol. 19 (1971) 145–154.
[56] G.W. Gross, L.M. Beidler, A quantitative analysis of isotope concentration profiles and rapid transport velocities in the C-fibers of the garfish olfactory nerve, J. Neurobiol. 6 (1975) 213–232.
[57] J. Gottofrey, H. Tjälve, Axonal transport of cadmium in the olfactory nerve of the pike, Pharmacol. Toxicol. 69 (1991) 242–252.
[58] R.G. Thorne, C.R. Emory, T.A. Ala, W.H. Frey, Quantitative analysis of the olfactory pathway for drug delivery to the brain, Brain Res. 692 (1995) 278–282.
[59] R.G. Thorne, G.J. Pronk, V. Padmanabhan, W.H. Frey, Delivery of insulin-like growth factor-I to the rat brain and spinal cord along olfactory and trigeminal pathways following intranasal administration, Neuroscience 127 (2004) 481–496.
[60] A.J. Darin De Lorenzo, The olfactory neuron and the blood-brain barrier, in: G.E. W. Wolstenholme, J. Knight (Eds.), Tast. Smell Vertebr., John Wiley & Sons, Ltd., Chichester, UK, 1970: pp. 151–176.
[61] Q. Liu, Y. Shen, J. Chen, X. Gao, C. Feng, L. Wang, Q. Zhang, X. Jiang, Nose-to-brain transport pathways of wheat germ agglutinin conjugated PEG-PLA nanoparticles, Pharm. Res. 29 (2012) 546–558.
[62] G. Oberdörster, A. Elder, A. Rinderknecht, Nanoparticles and the Brain: Cause for Concern? J. Nanosci. Nanotechnol. 9 (2009) 4996–5007.
[63] S. Maday, A.E. Twelvetrees, A.J. Moughamian, E.L.F. Holzbaur, Axonal transport: Cargo-specific mechanisms of motility and regulation, Neuron. 84 (2014) 292–309.
[64] Pál. Sigurdsson, T. Thorvaldsson, S. Gizurarson, E. Gunnarsson, Olfactory absorption of insulin to the brain, Drug Deliv. 4 (1997) 195–200.
[65] W.H. Frey, J. Liu, X. Chen, R.G. Thorne, J.R. Fawcett, T.A. Ala, Y.-E. Rahman, Delivery of 125 I-NGF to the brain via the olfactory route, Drug Deliv. 4 (1997) 87–92.
[66] Y. Wang, R. Aun, F.L.S. Tse, Brain uptake of dihydroergotamine after intravenous and nasal administration in the rat, Biopharm. Drug Dispos. 19 (1998) 571–575.
[67] K.J. Chou, M.D. Donovan, Lidocaine distribution into the CNS following nasal and arterial delivery: A comparison of local sampling and microdialysis techniques, Int. J. Pharm. 171 (1998) 53–61.
[68] M. Bagger, E. Bechgaard, A microdialysis model to examine nasal drug delivery and olfactory absorption in rats using lidocaine hydrochloride as a model drug, Int. J. Pharm. 269 (2004) 311–322.
[69] D. Garzotto, S. De Marchis, Quantum dot distribution in the olfactory epithelium after nasal delivery, in: 2010: pp. 118–123.
[70] L.R. Hanson, W.H. Frey, Intranasal delivery bypasses the blood-brain barrier to target therapeutic agents to the central nervous system and treat neurodegenerative disease, BMC Neurosci. 9 (2008) S5.
[71] N.J. Johnson, L.R. Hanson, W.H. Frey, Trigeminal pathways deliver a low molecular weight drug from the nose to the brain and orofacial structures, Mol. Pharm. 7 (2010) 884–893.
[72] M.L. Schaefer, B. Böttger, W.L. Silver, T.E. Finger, Trigeminal collaterals in the nasal epithelium and olfactory bulb: A potential route for direct modulation of olfactory information by trigeminal stimuli, J. Comp. Neurol. 444 (2002) 221–226.
[73] G. Brand, Olfactory/trigeminal interactions in nasal chemoreception, Neurosci. Biobehav. Rev. 30 (2006) 908–917.
[74] J.E. Cometto-Muñiz, C. Simons, Trigeminal chemesthesis, in: R.L. Doty (Ed.), Handb. Olfaction Gustation, 3rd ed., Wiley Blackwell, 2015.
[75] M.J.R. Ruigrok, E.C.M. de Lange, Emerging insights for translational pharmacokinetic and pharmacokinetic-pharmacodynamic studies: Towards prediction of nose-to-brain transport in humans, AAPS J. 17 (2015) 493–505.
[76] T.M. Ross, P.M. Martinez, J.C. Renner, R.G. Thorne, L.R. Hanson, W.H. Frey, Intranasal administration of interferon beta bypasses the blood-brain barrier to target the central nervous system and cervical lymph nodes: A non-invasive treatment strategy for multiple sclerosis, J. Neuroimmunol. 151 (2004) 66–77.
[77] F. Anton, P. Peppel, Central projections of trigeminal primary afferents innervating the nasal mucosa: A horseradish peroxidase study in the rat, Neuroscience. 41 (1991) 617–628.
[78] M. Johnston, A. Zakharov, C. Papaiconomou, G. Salmasi, D. Armstrong, Evidence of connections between cerebrospinal fluid and nasal lymphatic vessels in humans, non-human primates and other mammalian species, Cerebrospinal Fluid Res. 1 (2004), http://dx.doi.org/10.1186/1743-8454-1-2.
[79] B.J. Aungst, Absorption enhancers: Applications and advances, AAPS J. 14 (2012) 10–18.
[80] B.J. Bruno, G.D. Miller, C.S. Lim, Basics and recent advances in peptide and protein drug delivery, Ther. Deliv. 4 (2014) 1443–1467.
[81] B. Pavan, A. Dalpiaz, N. Ciliberti, C. Biondi, S. Manfredini, S. Vertuani, Progress in drug delivery to the central nervous system by the prodrug approach, Molecules. 13 (2008) 1035–1065.
[82] L. Juillerat-Jeanneret, F. Schmitt, Chemical modification of therapeutic drugs or drug vector systems to achieve targeted therapy: Looking for the grail, Med. Res. Rev. 27 (2007) 574–590.
[83] L. Yuan, J. Wang, W.-C. Shen, Lipidization of human interferon-alpha: A new approach toward improving the delivery of protein drugs, J. Control. Release. 129 (2008) 11–17.
[84] X. Yi, A.V. Kabanov, Brain delivery of proteins via their fatty acid and block copolymer modifications, J. Drug Target. 21 (2013) 940–955.
[85] K.C. Lee, M.O. Park, D.H. Na, Y.S. Youn, S.D. Lee, S.D. Yoo, H.S. Lee, P.P. DeLuca, Intranasal delivery of PEGylated salmon calcitonins: Hypocalcemic effects in rats, Calcif. Tissue Int. 73 (2003) 545–549.
[86] A. Abuchowski, J.R. McCoy, N.C. Palczuk, T. van Es, F.F. Davis, Effect of covalent attachment of polyethylene glycol on immunogenicity and circulating life of bovine liver catalase, J. Biol. Chem. 252 (1977) 3582–3586.
[87] A. Abuchowski, T. van Es, N.C. Palczuk, F.F. Davis, Alteration of immunological properties of bovine serum albumin by covalent attachment of polyethylene glycol, J. Biol. Chem. 252 (1977).

[88] G. Molineux, Pegylation: engineering improved pharmaceuticals for enhanced therapy, Cancer Treat. Rev. 28 (2002) 13–16.
[89] C.H. Huang, R. Kimura, R. Bawarshi-Nassar, A. Hussain, Mechanism of nasal absorption of drugs II: Absorption of L-tyrosine and the effect of structural modification on its absorption, J. Pharm. Sci. 74 (1985) 1298–1301.
[90] K. Morimoto, H. Yamaguchi, Y. Iwakura, M. Miyazaki, E. Nakatani, T. Iwamoto, Y. Ohashi, Y. Nakai, Effects of proteolytic enzyme inhibitors on the nasal absorption of vasopressin and an analogue, Pharm. Res. 8 (1991) 1175–1179.
[91] M.A. Sarkar, Drug metabolism in the nasal mucosa, Pharm. Res. 9 (1992) 1–9.
[92] V. Dhamankar, Cytochrome P450-mediated drug metabolizing activity in the nasal mucosa, The University of Iowa, Ph.D Dissertation, 2013.
[93] V.H.L. Lee, A. Yamamoto, Penetration and enzymatic barriers to peptide and protein absorption, 4 (1990) 171–207.
[94] A.L. Ungell, A. Andreasson, K. Lundin, L. Utter, Effects of enzymatic inhibition and increased paracellular shunting on transport of vasopressin analogues in the rat, J. Pharm. Sci. 81 (1992) 640–645.
[95] K. Morimoto, M. Miyazaki, M. Kakemi, Effects of proteolytic enzyme inhibitors on nasal absorption of salmon calcitonin in rats, Int. J. Pharm. 113 (1995) 1–8.
[96] A. Yamamoto, E. Hayakawa, V.H.L. Lee, Insulin and proinsulin proteolysis in mucosal homogenates of the albino rabbit: Implications in peptide delivery from nonoral routes, Life Sci. 47 (1990) 2465–2474.
[97] V.D. Hoang, A.R. Uchenna, J. Mark, K. Renaat, V. Norbert, Characterization of human nasal primary culture systems to investigate peptide metabolism, Int. J. Pharm. 238 (2002) 247–256.
[98] X. Duan, S. Mao, New strategies to improve the intranasal absorption of insulin, Drug Discov. Today. 15 (2010) 416–427.
[99] S. Mitragotri, P. Burke, R. Langer, Overcoming the challenges in administering biopharmaceuticals: formulation and delivery strategies, Nat. Rev. Drug Discov. 13 (2014) 655–672.
[100] S.S. Davis, L. Illum, Absorption enhancers for nasal drug delivery, Clin. Pharmacokinet. 42 (2003) 1107–1128.
[101] M. Miyamoto, H. Natsume, S. Iwata, K. Ohtake, M. Yamaguchi, D. Kobayashi, K. Sugibayashi, M. Yamashina, Y. Morimoto, Improved nasal absorption of drugs using poly-l-arginine: effects of concentration and molecular weight of poly-l-arginine on the nasal absorption of fluorescein isothiocyanate–dextran in rats, Eur. J. Pharm. Biopharm. 52 (2001) 21–30.
[102] H. Natsume, S. Iwata, K. Ohtake, M. Miyamoto, M. Yamaguchi, K.I. Hosoya, D. Kobayashi, K. Sugibayashi, Y. Morimoto, Screening of cationic compounds as an absorption enhancer for nasal drug delivery, Int. J. Pharm. 185 (1999) 1–12.
[103] J. Wang, S. Sakai, Y. Deguchi, D. Bi, Y. Tabata, K. Morimoto, Aminated gelatin as a nasal absorption enhancer for peptide drugs: evaluation of absorption enhancing effect and nasal mucosa perturbation in rats, J. Pharm. Pharmacol. 54 (2002) 181–188.
[104] L. Illum, Nasal drug delivery: New developments and strategies, Drug Discov. Today. 7 (2002) 1184–1189.
[105] M.M. Wen, Olfactory targeting through intranasal delivery of biopharmaceutical drugs to the brain - current development, Discov. Med. 11 (2011) 497–503.
[106] S.T. Charlton, S.S. Davis, L. Illum, Evaluation of effect of ephedrine on the transport of drugs from the nasal cavity to the systemic circulation and the central nervous system, J. Drug Target. 15 (2007) 370–377.
[107] P. Oliveira, A. Fortuna, G. Alves, A. Falcao, Drug-metabolizing enzymes and efflux transporters in nasal epithelium: Influence on the bioavailability of intranasally administered drugs, Curr. Drug Metab. 17 (7) (2016) 628–647.
[108] F.G. Hoosain, Y.E. Choonara, L.K. Tomar, P. Kumar, C. Tyagi, L.C. du Toit, V. Pillay, Bypassing P-Glycoprotein Drug Efflux Mechanisms: Possible Applications in Pharmacoresistant Schizophrenia Therapy, BioMed Research International (2015), Article ID 484963, 21 pages, http://dx.doi.org/10.1155/2015/484963.
[109] P.G. Djupesland, Nasal drug delivery devices: Characteristics and performance in a clinical perspective-a review, Drug Deliv. Transl. Res. 3 (2013) 42–62.
[110] C.V. Pardeshi, Y.H. Vanjari, Novel nasal devices for the efficient drug delivery: A systemic review, Indian J. Nov. Drug Deliv. 7 (2015) 1–9.
[111] Kurve Technology, Controlled Particle Dispersion - Versatile Liquid Drug Delivery, http://www.kurvetech.com.
[112] T. Sullivan, J. Durham, Dose Dispensing Containers, US Patent 9,248,076 B2 (Feb. 2, 2016).
[113] Mystic Pharmaceuticals, Nose to Brain Delivery Systems, http://mysticpharmaceuticals.com/nose-to-brain-delivery/.
[114] J.D. Hoekman, M. Hite, A. Brunelle, J. Relethford, R.J.Y. Ho, Nasal Drug Delivery Device, US9550036 B2 (Jan. 24, 2017).
[115] SipNose, Nasal Delivery Systems, https://www.sipnose.com.
[116] Optinose, http://www.optinose.com.
[117] M. van Woensel, N. Wauthoz, R. Rosière, K. Amighi, V. Mathieu, F. Lefranc, S. van Gool, S. de Vleeschouwer, Formulations for intranasal delivery of pharmacological agents to combat brain disease: A new opportunity to tackle GBM? Cancers (Basel). 5 (2013) 1020–1048.
[118] C.-T. Lu, Y.-Z. Zhao, H.L. Wong, J. Cai, L. Peng, X.-Q. Tian, Current approaches to enhance CNS delivery of drugs across the brain barriers, Int. J. Nanomedicine. 9 (2014) 2241–2257.
[119] E. Muntimadugu, R. Dhommati, A. Jain, V.G.S. Challa, M. Shaheen, W. Khan, Intranasal delivery of nanoparticle encapsulated tarenflurbil: A potential brain targeting strategy for Alzheimer's disease, Eur. J. Pharm. Sci. 92 (2016) 224–234.
[120] H. Xia, X. Gao, G. Gu, Z. Liu, N. Zeng, Q. Hu, Q. Song, L. Yao, Z. Pang, X. Jiang, J. Chen, H. Chen, Low molecular weight protamine-functionalized nanoparticles for drug delivery to the brain after intranasal administration, Biomaterials 32 (2011) 9888–9898.
[121] A.S. Hanafy, R.M. Farid, S.S. Elgamal, Complexation as an approach to entrap cationic drugs into cationic nanoparticles administered intranasally for Alzheimer's disease management: Preparation and detection in rat brain, Drug Dev. Ind. Pharm. 41 (2015) 2055–2068.
[122] S. Alam, Z.I. Khan, G. Mustafa, M. Kumar, F. Islam, A. Bhatnagar, F.J. Ahmad, Development and evaluation of thymoquinone-encapsulated chitosan nanoparticles for nose-to-brain targeting : a pharmacoscintigraphic study, (2012) 5705–5718.
[123] S. Di Gioia, A. Trapani, D. Mandracchia, E. De Giglio, S. Cometa, V. Mangini, F. Arnesano, G. Belgiovine, S. Castellani, L. Pace, M. Angelo Lavecchia, G. Trapani, M. Conese, G. Puglisi, T. Cassano, Intranasal delivery of dopamine to the striatum using glycol chitosan/sulfobutylether-β-cyclodextrin based nanoparticles, Eur. J. Pharm. Biopharm. 94 (2015) 180–193.
[124] D. Patel, S. Naik, K. Chuttani, R. Mathur, A.K. Mishra, A. Misra, Intranasal delivery of cyclobenzaprine hydrochloride-loaded thiolated chitosan nanoparticles for pain relief, J. Drug Target. 21 (2013) 759–769.
[125] D. Patel, S. Naik, A. Misra, Improved transnasal transport and brain uptake of tizanidine HCl-loaded thiolated chitosan nanoparticles for alleviation of pain, J. Pharm. Sci. 101 (2012) 690–706.
[126] A. Dalpiaz, E. Gavini, G. Colombo, P. Russo, F. Bortolotti, L. Ferraro, S. Tanganelli, A. Scatturin, E. Menegatti, P. Giunchedi, Brain uptake of an anti-ischemic agent by nasal administration of microparticles, J. Pharm. Sci. 97 (2008) 4889–4903.
[127] G. Rassu, E. Soddu, M. Cossu, A. Brundu, G. Cerri, N. Marchetti, L. Ferraro, R.F. Regan, P. Giunchedi, E. Gavini, A. Dalpiaz, Solid microparticles based on chitosan or methyl-β-cyclodextrin: A first formulative approach to increase the nose-to-brain transport of deferoxamine mesylate, J. Control. Release. 201 (2015) 68–77.
[128] S. Haque, S. Md, J.K. Sahni, J. Ali, S. Baboota, Development and evaluation of brain targeted intranasal alginate nanoparticles for treatment of depression, J. Psychiatr. Res. 48 (2014) 1–12.
[129] Z. Liu, M. Jiang, T. Kang, D. Miao, G. Gu, Q. Song, L. Yao, Q. Hu, Y. Tu, Z. Pang, H. Chen, X. Jiang, X. Gao, J. Chen, Lactoferrin-modified PEG-co-PCL nanoparticles for enhanced brain delivery of NAP peptide following intranasal administration, Biomaterials 34 (2013) 3870–3881.
[130] F.N. Fonseca, A.H. Betti, F.C. Carvalho, M.P.D. Gremião, F.A. Dimer, S.S. Guterres, M.L. Tebaldi, S.M.K. Rates, A.R. Pohlmann, Mucoadhesive amphiphilic methacrylic copolymer-functionalized poly(ε-caprolactone) nanocapsules for nose-to-brain delivery of olanzapine, J. Biomed. Nanotechnol. 11 (2015) 1472–1481.
[131] S.B. Yarragudi, R. Richter, H. Lee, G.F. Walker, A.N. Clarkson, H. Kumar, S.B. Rizwan, Formulation of olfactory-targeted microparticles with tamarind seed polysaccharide to improve nose-to-brain transport of drugs, Carbohydr. Polym. 163 (2017) 216–226.
[132] A. Mistry, The development and application of biological models for evaluation of direct nose-to-brain drug delivery systems. Ph.D Dissertation, University of Nottingham, (2009).
[133] A. Mistry, S.Z. Glud, J. Kjems, J. Randel, K.A. Howard, S. Stolnik, L. Illum, Effect of physicochemical properties on intranasal nanoparticle transit into murine olfactory epithelium, J. Drug Target. 17 (2009) 543–552.
[134] G.A. Abdelbary, M.I. Tadros, Brain targeting of olanzapine via intranasal delivery of core-shell difunctional block copolymer mixed nanomicellar carriers: In vitro characterization, ex vivo estimation of nasal toxicity and in vivo biodistribution studies, Int. J. Pharm. 452 (2013) 300–310.
[135] T. Kanazawa, F. Akiyama, S. Kakizaki, Y. Takashima, Y. Seta, Delivery of siRNA to the brain using a combination of nose-to-brain delivery and cell-penetrating peptide-modified nano-micelles, Biomaterials 34 (2013) 9220–9226.
[136] G. Rassu, E. Soddu, A.M. Posadino, G. Pintus, B. Sarmento, P. Giunchedi, E. Gavini, Nose-to-brain delivery of BACE1 siRNA loaded in solid lipid nanoparticles for Alzheimer's therapy, Colloids Surfaces B Biointerfaces 152 (2017) 296–301.
[137] O. Gartziandia, E. Herran, J.L. Pedraz, E. Carro, M. Igartua, R.M. Hernandez, Chitosan coated nanostructured lipid carriers for brain delivery of proteins by intranasal administration, Colloids Surfaces B Biointerfaces 134 (2015) 304–313.
[138] H.A. Salama, A.A. Mahmoud, A.O. Kamel, M. Abdel Hady, G.A.S. Awad, Phospholipid based colloidal poloxamer-nanocubic vesicles for brain targeting via the nasal route, Colloids Surfaces B Biointerfaces 100 (2012) 146–154.
[139] M. Kumar, A. Misra, A.K. Babbar, A.K. Mishra, P. Mishra, K. Pathak, Intranasal nanoemulsion based brain targeting drug delivery system of risperidone, Int. J. Pharm. 358 (2008) 285–291.
[140] C. Yu, P. Gu, W. Zhang, C. Cai, H. He, X. Tang, Evaluation of submicron emulsion as vehicles for rapid-onset intranasal delivery and improvement in brain targeting of zolmitriptan, Drug Deliv. 18 (2011) 578–585.
[141] V.V. Jogani, P.J. Shah, P. Mishra, A.K. Mishra, A.R. Misra, Intranasal mucoadhesive microemulsion of tacrine to improve brain targeting, Alzheimer Dis. Assoc. Disord. 22 (2008) 116–124.
[142] S. Sharma, S. Lohan, R.S.R. Murthy, Formulation and characterization of intranasal mucoadhesive nanoparticulates and thermo-reversible gel of levodopa for brain delivery, Drug Dev. Ind. Pharm. 40 (2014) 869–878.
[143] M.A.K. Greco, W.H. Frey II, J. DeRose, R.B. Matthews, L.R. Bresin Hanson, Intranasal Delivery of Modafinil, US7,989,502B2 (Aug. 2, 2011).
[144] J. Sanchez-Ramos, V. Sava, S. Song, S.S. Mohapatra, S. Mohapatra, Manganese Ion Coated Nanoparticles for Delivery of Compositions Into the Central Nervous System by Nasal Insufflation, US9,375,400B2 (Jun. 28, 2016).
[145] O. Kammona, C. Kiparissides, Recent advances in nanocarrier-based mucosal delivery of biomolecules, J. Control. Release. 161 (2012) 781–794.
[146] J.H. Adair, M.P. Parette, E.I. Altinoğlu, M. Kester, Nanoparticulate alternatives for drug delivery, ACS Nano. 4 (2010) 4967–4970.
[147] E. Samaridou, M.J. Alonso, Nose-to-brain peptide delivery - The potential of nanotechnology, Bioorganic Med, Chem, 2017.

[148] U. Seju, A. Kumar, K.K. Sawant, Development and evaluation of olanzapine-loaded PLGA nanoparticles for nose-to-brain delivery: In vitro and in vivo studies, Acta Biomater. 7 (2011) 4169–4176.
[149] J. Chen, C. Zhang, Q. Liu, X. Shao, C. Feng, Y. Shen, Q. Zhang, X. Jiang, Solanum tuberosum lectin-conjugated PLGA nanoparticles for nose-to-brain delivery: In vivo and in vitro evaluations, J. Drug Target. 20 (2012) 174–184.
[150] C. Zhang, J. Chen, C. Feng, X. Shao, Q. Liu, Q. Zhang, Z. Pang, X. Jiang, Intranasal nanoparticles of basic fibroblast growth factor for brain delivery to treat Alzheimer's disease, Int. J. Pharm. 461 (2014) 192–202.
[151] Z. Wen, Z. Yan, K. Hu, Z. Pang, X. Cheng, L. Guo, Q. Zhang, X. Jiang, L. Fang, R. Lai, Odorranalectin-conjugated nanoparticles: Preparation, brain delivery and pharmacodynamic study on Parkinson's disease following intranasal administration, J. Control. Release. 151 (2011) 131–138.
[152] X. Gao, B. Wu, Q. Zhang, J. Chen, J. Zhu, W. Zhang, Z. Rong, H. Chen, X. Jiang, Brain delivery of vasoactive intestinal peptide enhanced with the nanoparticles conjugated with wheat germ agglutinin following intranasal administration, J. Control. Release. 121 (2007) 156–167.
[153] X. Gao, J. Chen, W. Tao, J. Zhu, Q. Zhang, H. Chen, X. Jiang, UEA I-bearing nanoparticles for brain delivery following intranasal administration, Int. J. Pharm. 340 (2007) 207–215.
[154] M. Fazil, S. Md, S. Haque, M. Kumar, S. Baboota, J.K. Sahni, J. Ali, Development and evaluation of rivastigmine loaded chitosan nanoparticles for brain targeting, Eur. J. Pharm. Sci. 47 (2012) 6–15.
[155] S. Md, R.A. Khan, G. Mustafa, K. Chuttani, S. Baboota, J.K. Sahni, J. Ali, Bromocriptine loaded chitosan nanoparticles intended for direct nose to brain delivery: Pharmacodynamic, Pharmacokinetic and Scintigraphy study in mice model, Eur. J. Pharm. Sci. 48 (2013) 393–405.
[156] A.M. Al-Ghananeem, H. Saeed, R. Florence, R.A. Yokel, A.H. Malkawi, Intranasal drug delivery of didanosine-loaded chitosan nanoparticles for brain targeting an attractive route against infections caused by aids viruses, J. Drug Target. 18 (2010) 381–388.
[157] X. Wang, N. Chi, X. Tang, Preparation of estradiol chitosan nanoparticles for improving nasal absorption and brain targeting, Eur. J. Pharm. Biopharm. 70 (2008) 735–740.
[158] M. Kumar, R.S. Pandey, K.C. Patra, S.K. Jain, M.L. Soni, J.S. Dangi, J. Madan, Evaluation of neuropeptide loaded trimethyl chitosan nanoparticles for nose to brain delivery, Int. J. Biol. Macromol. 61 (2013) 189–195.
[159] E. Gavini, G. Rassu, L. Ferraro, A. Generosi, J.V. Rau, A. Brunetti, P. Giunchedi, A. Dalpiaz, Influence of chitosan glutamate on the in vivo intranasal absorption of rokitamycin from microspheres, J. Pharm. Sci. 100 (2011) 1488–1502.
[160] S. Patel, S. Chavhan, H. Soni, A.K. Babbar, R. Mathur, A.K. Mishra, K. Sawant, Brain targeting of risperidone-loaded solid lipid nanoparticles by intranasal route, J. Drug Target. 19 (2011) 468–474.
[161] Y.Z. Zhao, X. Li, C.T. Lu, M. Lin, L.J. Chen, Q. Xiang, M. Zhang, R.R. Jin, X. Jiang, X.T. Shen, X.K. Li, J. Cai, Gelatin nanostructured lipid carriers-mediated intranasal delivery of basic fibroblast growth factor enhances functional recovery in hemiparkinsonian rats, Nanomed. Nanotechnol. Biol. Med. 10 (2014) 755–764.
[162] Z.Z. Yang, Y.Q. Zhang, Z.Z. Wang, K. Wu, J.N. Lou, X.R. Qi, Enhanced brain distribution and pharmacodynamics of rivastigmine by liposomes following intranasal administration, Int. J. Pharm. 452 (2013) 344–354.
[163] J.D. Hoekman, P. Srivastava, R.J.Y. Ho, Aerosol-stable peptide-coated liposome nanoparticles: A proof-of-concept study with opioid fentanyl in enhancing analgesic effects and reducing plasma drug exposure, J. Pharm. Sci. 103 (2014) 2231–2239.
[164] H.A. Salama, A.A. Mahmoud, A.O. Kamel, M. Abdel Hady, G.A.S. Awad, Brain delivery of olanzapine by intranasal administration of transfersomal vesicles, J. Liposome Res. 22 (2012) 336–345.
[165] M. Boche, V. Pokharkar, Quetiapine nanoemulsion for intranasal drug delivery: evaluation of brain-targeting efficiency, AAPS PharmSciTech. 18 (2017) 686–696.
[166] H.S. Mahajan, M.S. Mahajan, P.P. Nerkar, A. Agrawal, Nanoemulsion-based intranasal drug delivery system of saquinavir mesylate for brain targeting, Drug Deliv. 21 (2014) 148–154.
[167] M. Kumar, A. Misra, A.K. Mishra, P.P. Mishra, K. Pathak, Mucoadhesive nanoemulsion-based intranasal drug delivery system of olanzapine for brain targeting, J. Drug Target. 16 (2008) 806–814.
[168] G. Sharma, A.K. Mishra, P. Mishra, A. Misra, Intranasal cabergoline: pharmacokinetic and pharmacodynamic studies, AAPS PharmSciTech. 10 (2009) 1321–1330.
[169] K. Florence, L. Manisha, B.A. Kumar, K. Ankur, M.A. Kumar, M. Ambikanandan, Intranasal clobazam delivery in the treatment of status epilepticus, J. Pharm. Sci. 100 (2011) 692–703.
[170] H. Bshara, R. Osman, S. Mansour, A.E.H.A. El-Shamy, Chitosan and cyclodextrin in intranasal microemulsion for improved brain buspirone hydrochloride pharmacokinetics in rats, Carbohydr. Polym. 99 (2014) 297–305.
[171] E. Sekerdag, S. Lüle, S. Bozdağ Pehlivan, N. Öztürk, A. Kara, A. Kaffashi, I. Vural, I. Işıkay, B. Yavuz, K.K. Oguz, F. Söylemezoğlu, Y. Gürsoy-Özdemir, M. Mut, A potential non-invasive glioblastoma treatment: Nose-to-brain delivery of farnesylthiosalicylic acid incorporated hybrid nanoparticles, J. Control. Release. 261 (2017) 187–198.
[172] S. Lungare, K. Hallam, R.K.S. Badhan, Phytochemical-loaded mesoporous silica nanoparticles for nose-to-brain olfactory drug delivery, Int. J. Pharm. 513 (2016) 280–293.
[173] R. Pathak, R. Prasad Dash, M. Misra, M. Nivsarkar, Role of mucoadhesive polymers in enhancing delivery of nimodipine microemulsion to brain via intranasal route, Acta Pharm. Sin. B. 4 (2014) 151–160.
[174] M.C. Chen, K. Sonaje, K.J. Chen, H.W. Sung, A review of the prospects for polymeric nanoparticle platforms in oral insulin delivery, Biomaterials 32 (2011) 9826–9838.
[175] R.C. Mundargi, V.R. Babu, V. Rangaswamy, P. Patel, T.M. Aminabhavi, Nano/micro technologies for delivering macromolecular therapeutics using poly(d, l-lactide-co-glycolide) and its derivatives, J. Control. Release. 125 (2008) 193–209.
[176] N. Csaba, M. Garcia-Fuentes, M.J. Alonso, Nanoparticles for nasal vaccination, Adv. Drug Deliv. Rev. 61 (2009) 140–157.
[177] S. Sharma, T.K.S. Mukkur, H.A.E. Benson, Y. Chen, Pharmaceutical aspects of intranasal delivery of vaccines using particulate systems, J. Pharm. Sci. 98 (2009) 812–843.
[178] A. Bernkop-Schnürch, M. Hornof, D. Guggi, Thiolated chitosans, Eur. J. Pharm. Biopharm. 57 (2004) 9–17.
[179] Q. Gan, T. Wang, Chitosan nanoparticle as protein delivery carrier-Systematic examination of fabrication conditions for efficient loading and release, Colloids Surfaces B Biointerfaces. 59 (2007) 24–34.
[180] C. Bulmer, A. Margaritis, A. Xenocostas, Production and characterization of novel chitosan nanoparticles for controlled release of rHu-Erythropoietin, Biochem. Eng. J. 68 (2012) 61–69.
[181] S. Haque, S. Md, M. Fazil, M. Kumar, J.K. Sahni, J. Ali, S. Baboota, Venlafaxine loaded chitosan NPs for brain targeting: Pharmacokinetic and pharmacodynamic evaluation, Carbohydr. Polym. 89 (2012) 72–79.
[182] T.K. Dash, V.B. Konkimalla, Poly-ε-caprolactone based formulations for drug delivery and tissue engineering: A review, J. Control. Release. 158 (2012) 15–33.
[183] C. Kiparissides, O. Kammona, Nanoscale carriers for targeted delivery of drugs and therapeutic biomolecules, Can. J. Chem. Eng. 91 (2013) 638–651.
[184] S.A. Chime, I.V. Onyishi, Lipid-based drug delivery systems (LDDS): Recent advances and applications of lipids in drug delivery, African J. Pharm. Pharmacol. 7 (2013) 3034–3059.
[185] G. Fricker, T. Kromp, A. Wendel, A. Blume, J. Zirkel, H. Rebmann, C. Setzer, R.O. Quinkert, F. Martin, C. Müller-Goymann, Phospholipids and lipid-based formulations in oral drug delivery, Pharm. Res. 27 (2010) 1469–1486.
[186] M. Muchow, P. Maincent, R.H. Müller, Lipid nanoparticles with a solid matrix (SLN®, NLC®, LDC®) for oral drug delivery, Drug Dev. Ind. Pharm. 34 (2008) 1394–1405.
[187] H. Harde, M. Das, S. Jain, Solid lipid nanoparticles: an oral bioavailability enhancer vehicle, Expert Opin. Drug Deliv. 8 (2011) 1407–1424.
[188] S. Martins, B. Sarmento, D.C. Ferreira, E.B. Souto, Lipid-based colloidal carriers for peptide and protein delivery - Liposomes versus lipid nanoparticles, Int. J. Nanomedicine. 2 (2007) 595–607.
[189] A.J. Almeida, E. Souto, Solid lipid nanoparticles as a drug delivery system for peptides and proteins, Adv. Drug Deliv. Rev. 59 (2007) 478–490.
[190] S.A. Wissing, O. Kayser, R.H. Müller, Solid lipid nanoparticles for parenteral drug delivery, Adv. Drug Deliv. Rev. 56 (2004) 1257–1272.
[191] R.H. Müller, M. Radtke, S.A. Wissing, Nanostructured lipid matrices for improved microencapsulation of drugs, Int. J. Pharm. 242 (2002) 121–128.
[192] T. Karamanidou, V. Bourganis, O. Kammona, C. Kiparissides, Lipid-based nanocarriers for the oral administration of biopharmaceutics, Nanomedicine. 11 (2016) 3009–3032.
[193] J. Zhang, Novel emulsion-based delivery systems, University of Minnesota, Ph.D, Disssertation, 2011.
[194] H. Marino, Phase inversion temperature emulsification: From batch to continuous process, University of Bath, 2010.
[195] K. Meleson, The formation and stability of nanoemulsions, University of California, Ph.D, Disssertation, 2008.
[196] D.J. McClements, Nanoemulsions versus microemulsions: terminology, differences, and similarities, Soft Matter. 8 (2012) 1719–1729.
[197] J.F. Correia-Pinto, N. Csaba, M.J. Alonso, Vaccine delivery carriers: Insights and future perspectives, Int. J. Pharm. 440 (2013) 27–38.
[198] P.M. Ved, K. Kim, Poly(ethylene oxide/propylene oxide) copolymer thermo-reversible gelling system for the enhancement of intranasal zidovudine delivery to the brain, Int. J. Pharm. 411 (2011) 1–9.
[199] V.S.S. Gonçalves, A.A. Matias, J. Poejo, A.T. Serra, C.M.M. Duarte, Application of RPMI 2650 as a cell model to evaluate solid formulations for intranasal delivery of drugs, Int. J. Pharm. 515 (2016) 1–10.
[200] O. Gartziandia, S.P. Egusquiaguirre, J. Bianco, J.L. Pedraz, M. Igartua, R.M. Hernandez, V. Préat, A. Beloqui, Nanoparticle transport across in vitro olfactory cell monolayers, Int. J. Pharm. 499 (2016) 81–89.
[201] N. Islam, M.J. Cleary, Developing an efficient and reliable dry powder inhaler for pulmonary drug delivery – a review for multidisciplinary researchers, Med. Eng. Phys. 34 (2012) 409–427.
[202] H.R. Costantino, L. Illum, G. Brandt, P.H. Johnson, S.C. Quay, Intranasal delivery: physicochemical and therapeutic aspects, Int. J. Pharm. 337 (1–2) (2007) 1–24.
[203] K. Inthavong, Q. Ge, C.M.K. Se, W. Yang, J.Y. Tu, Simulation of sprayed particle deposition in a human nasal cavity including a nasal spray device, J. Aerosol Sci. 42 (2) (2011) 100–113.
[204] D.J. Doorly, D.J. Taylor, R.C. Schroter, Mechanics of airflow in the human nasal airways, Respiratory Physiology and Neurobiology 163 (1–3) (2008) 100–110.
[205] H. Shi, C. Kleinstreuer, Z. Zhang, Laminar airflow and nanoparticle or vapor deposition in a human nasal cavity model, J. Biomech. Eng. 128 (5) (2006) 697–706.
[206] J.M.G. Guilherme, J.D. Schroeter, J.S. Kimbell, Olfactory deposition of inhaled nanoparticles in humans, Inhalation Toxicol. 27 (8) (2015) 394–403.
[207] L. Tian, Y. Shang, J. Dong, K. Inthavong, J. Tu, Human nasal olfactory deposition of inhaled nanoparticles at low to moderate breathing rate, J. Aerosol. Sci. 113 (2017) 189–200.
[208] J. Wen, K. Inthavong, J.Y. Tu, S. Wang, Numerical simulations for detailed airflow dynamics in a human nasal cavity, Respir. Physiol. Neurobiol. 161 (2) (2008)

125–135.
[209] Y. Liu, E.A. Matida, J. Gu, M.R. Johnson, Numerical simulation of aerosol deposition in a 3-D human nasal cavity using RANS, RANS/EIM, and LES, J. Aerosol. Sci. 38 (7) (2007) 683–700.
[210] P.W. Longest, L.T. Holbrook, In silico models of aerosol delivery to the respiratory tract-developments and applications, Adv. Drug Deliv. Rev. 64 (2011) 296–311.
[211] K. Inthavong, K. Zhang, J. Tu, Modelling submicron and micron particle deposition in a human nasal cavity, Seventh International Conference on CFD in the Minerals and Process Industries, CSIRO, Melbourne, Australia, 2009.
[212] N.A. Peppas, P.A. Buri, Surface, interfacial and molecular aspects of polymer bioadhesion on soft tissues, J. Control. Release 2 (1984) 257–275.
[213] A.N.F. Versypt, D.W. Pack, R.D. Braatz, Mathematical modeling of drug delivery from autocatalytically degradable PLGA microspheres — A review, J. Control. Release 165 (2013) 29–37.
[214] S. Fredenberg, M. Wahlgren, M. Reslow, A. Axelsson, The mechanisms of drug release in poly(lactic-co-glycolic acid)-based drug delivery systems–a review, Int. J. Pharm. 415 (1–2) (2011) 34–52.
[215] V. Kanellopoulos, E. Tsiliopoulou, G. Dompazis, V. Touloupides, C. Kiparissides, Evaluation of the internal particle morphology in catalytic gas-phase olefin polymerization reactors, Ind. Eng. Chem. Res. 46 (2007) 1928–1937.
[216] G. Grassi, M. Grassi, Mathematical modeling of nanocrystalline and amorphous drugs release and gastro-intestinal absorption from polymeric particles, Clustering Algorithms and Applications, Mathematical Modeling, 2011, pp. 49–82.
[217] A. Zhao, V.G.J. Rodgers, Using TEM to couple transient protein distribution and release for PLGA microparticles for potential use as vaccine delivery vehicles, J. Control. Release 113 (2006) 15–22.
[218] Y. Cu, W.M. Saltzman, Mathematical modeling of molecular diffusion through mucus, Adv. Drug Deliv. 61 (2) (2009) 101–114.
[219] M. Ernst, T. John, M. Guenther, C. Wagner, U.F. Schaefer, C.M. Lehr, A Model for the transient subdiffusive behavior of particles in mucus, Biophys. J. 112 (1) (2017) 172–179.
[220] S. Riniker, J.R. Allison, W.F. van Gunsteren WF, On developing coarse-grained models for biomolecular simulation: a review. Phys. Chem. Chem. Phys. 14 (36) (2012) 12423–12430.
[221] P. Gniewek, A. Kolinski, Coarse-grained modeling of mucus barrier properties, Biophys. J. 102 (2012) 195–200.
[222] J. Wang, X. Shi, Molecular dynamics simulation of diffusion of nanoparticles in mucus, Acta Mech. Solida Sinica (2017), http://dx.doi.org/10.1016/j.camss.2017.03.012.
[223] G. Hu, B. Jiao, X. Shi, R.P. Valle, Q. Fan, Y.Y. Zuo, Physicochemical properties of nanoparticles regulate translocation across pulmonary surfactant monolayer and formation of lipoprotein corona, ACS Nano 7 (12) (2013) 10525–10533.
[224] M. Feig, I. Yu, P.H. Wang, G. Nawrocki, Y. Sugita, Crowding in cellular environments at an atomistic level from computer simulations, J. Phys. Chem. B. 121 (34) (2017) 8009–8025.
[225] M.G. Saunders, G.A. Voth, Coarse-graining methods for computational biology, Annu. Rev. Biophys. 42 (2013) 73–93.
[226] M. Feig, Y. Sugita, Reaching new levels of realism in modeling biological macromolecules in cellular environments, J. Mol. Graph. Model. 45 (2013) 144–156.
[227] M. Lundqvist, J. Stigler, G. Elia, I. Lynch, T. Cedervall, K.A. Dawson, Nanoparticle size and surface properties determine the protein corona with possible implications for biological impacts, PNAS 105 (38) (2008) 14265–14270.
[228] Q. Hu, X. Bai, G. Hu, Y.Y. Zuo, Unveiling the molecular structure of pulmonary surfactant corona on nanoparticles, ACS Nano 11 (7) (2017) 6832–6842.
[229] T. Ando, I. Yu, M. Feig, Y. Sugita, Thermodynamics of macromolecular association in heterogeneous crowding environments: theoretical and simulation studies with a simplified model, J. Phys. Chem. B 120 (2016) 11856–11865.
[230] D. Gnutt, S. Ebbinghaus, The macromolecular crowding effect from in vitro into the cell, Biol. Chem. 397 (2016) 37–44.
[231] H.X. Zhou, G. Rivas, A.P. Minton, Macromolecular, crowding and confinement: biochemical, biophysical, and potential physiological consequences, Annu. Rev. Biophys. 37 (2008) 375–397.
[232] T. Ando, J. Skolnick, Crowding and hydrodynamic interactions likely dominate in vivo macromolecular motion, Proc. Natl. Acad. Sci. 26;107(43) (2010) 18457–18462.
[233] H.M. Ding, W.D. Tian, Y.Q. Ma, Designing nanoparticle translocation through membranes by computer simulations, ACS Nano 6 (2) (2012) 1230–1238.
[234] B. Jing, R.C.T. Abot, Y. Zhu, Semihydrophobic nanoparticle-induced disruption of supported lipid bilayers: specific ion effect, J. Phys. Chem. B 118 (2014) 13175–13182.
[235] H.M. Jones, Y. Chen, C. Gibson, T. Heimbach, N. Parrott, S.A. Peters, J. Snoeys, V.V. Upreti, M. Zheng, S.D. Hall, Physiologically based pharmacokinetic modeling in drug discovery and development: a pharmaceutical industry perspective, Clin. Pharmacol. Ther. 97 (2015) 247–262.
[236] R.F. Phalen, O.G. Raabe, The evolution of inhaled particle dose modeling: A review, J. Aerosol Sci. 99 (2016) 7–13.
[237] A. Vulović, T. Šušteršič, S. Cvijić, S. Ibrić, N. Filipović, Coupled in silico platform: Computational fluid dynamics (CFD) and physiologically-based pharmacokinetic (PBPK) modelling, Eur. J. Pharm. Sci. 113 (2018) 171–184.